



Efficient simulation methods for the Quasi-Gaussian term-structure model with volatility smiles: practical applications of the KLVN-scheme★

Yuji Shinozaki


To cite this article: Yuji Shinozaki (2021) Efficient simulation methods for the Quasi-Gaussian term-structure model with volatility smiles: practical applications of the KLVN-scheme★, Quantitative Finance, 21:7, 1147-1161, DOI: [10.1080/14697688.2020.1861320](https://doi.org/10.1080/14697688.2020.1861320)

To link to this article: <https://doi.org/10.1080/14697688.2020.1861320>



Published online: 04 Feb 2021.



Submit your article to this journal 



Article views: 98



View related articles 



View Crossmark data 

Efficient simulation methods for the Quasi-Gaussian term-structure model with volatility smiles: practical applications of the KLVN-scheme★

YUJI SHINOZAKI*†‡§

†Quantitative Analytics & Development, SMBC Nikko Securities Inc, 1-5-1 Marunouchi, Chiyoda-ku, 100-6590 Tokyo, Japan

‡Tokyo Institute of Technology, 2-12-1 Ookayama, Meguro-ku, 152-8552 Tokyo, Japan

(Received 14 April 2020; accepted 27 November 2020; published online 4 February 2021)

This paper considers computational challenges to practically important problems related to pricing exotic interest rate derivatives, using the Kusuoka–Lyons–Ninomiya–Victoir scheme (KLVN-scheme) which is a higher-order discretization framework for performing weak approximations of stochastic differential equations. The author demonstrates the KLVN-scheme is even more effective for some types of practical high-dimensional problems, especially when close or approximate solutions to the involved ordinary differential equations can be found. Moreover, the numerical results show the proposed methods are 500 to more than 6000 times faster compared to the conventional methods.

Keywords: Computational finance; Term-structure model; Short rate model; Stochastic volatility model; Higher-order discretization method; KLVN-scheme; Quasi-Monte Carlo method

JEL Classifications: C63, G12

1. Introduction

1.1. Background

1.1.1. Interest rate term-structure modeling. In pricing and hedging exotic interest rate derivatives (e.g. options on general swaps, callable bonds, or path-dependent options), it is necessary to model the dynamics of the entire yield curve. In 1992, the Heath–Jarrow–Morton framework (HJM model) was proposed in Heath *et al.* (1992) as a general setting to model the evolution of the forward curve. Since then, many models have been proposed using the HJM framework; they are classified into three categories: the short rate model (Gaussian HJM model), the Libor/Swap market model (Brace *et al.* 1997), and the Markov functional model (Hunt *et al.* 2000). Although models belonging to the second and third categories provide better fits to the volatility smiles, the short rate model, which is the most traditional, is getting more

common in the financial industry recently, mainly because of its simplicity, consistency with the x -valuation adjustment calculation (Green 2015, Gregory 2015), and the end of Libor (UK Financial Conduct Authority 2019). Therefore, we focus on the short rate model, particularly on the quasi-Gaussian term-structure models.

1.1.2. Simulation problem of quasi-Gaussian term-structure model. Restricting the HJM model dynamics to Markovian form by specifying the volatility functions of the HJM model, some researchers independently proposed the quasi-Gaussian term-structure models (qG model), which is also called the Cheyette model or the pseudo-Gaussian model, in Jamshidian (1991), Cheyette (1991) and Ritchken and Sankarasubramanian (1995). Note that the quasi-Gaussian term-structure model, which is a quite general model class, covers the traditional short rate models such as the Vasicek

*Corresponding author. Email: sinozaki.yuji@gmail.com

★The views expressed in this paper are those of the author and do not necessarily reflect the official views of the affiliated institutions of the author.

§Current affiliation: Bank of Japan, 2-1-1 Nihonbashi-Hongokuchō, Chuo-ku, Tokyo 103-0021, Japan

This article has been corrected with minor changes. These changes do not impact the academic content of the article.

model (Vasicek 1977), the Ho–Lee model (Ho and Lee 1986), and the Hull–White model (Hull and White 1990). The literature on the qG model is abundant; in particular, some studies have been conducted from practical perspectives (Andreasen 2001, 2010, Beyna 2013). Refer to Chapter 13 of Anderson and Piterbarg (2010) for the issues in practical use, such as calibration procedures, explicit formulas for pricing Swaptions/Caps, and numerical methods.

Let $P(t, T)$ denote the time t price of a zero-coupon bond delivering for certain \$1 at maturity $T > t$. In interest rate term-structure modeling, given the initial yield curve $\{P(t_0, T)\}_{t_0 < T}$ at time t_0 , we aim to model the dynamics of the entire yield curve $\{P(t, T)\}_{t_0 < t < T}$. Let $r(t)$ denote the short rate and $f(t, T)$ the forward (i.e. $r(t) = \lim_{T \downarrow t} -\frac{\log P(t, T)}{T-t}$, $f(t, T) = -\frac{\partial}{\partial s} \log P(t, s)|_{s=T}$). The qG models describe the dynamics of $r(t) - f(0, t)$ using the stochastic factors $(x^{(1)}(t), x^{(2)}(t), \dots, x^{(l)}(t))$ that follow specific stochastic differential equations (SDEs). Hence, to calculate the prices of exotic interest rate derivatives using the qG model, one has to calculate expectations of form $E[\sum_{i=1}^K F_i(x^{(1)}(s_i), x^{(2)}(s_i), \dots, x^{(l)}(s_i))]$ where $F_i: \mathbb{R}^l \rightarrow \mathbb{R}$. There are two major methods to calculate these expectations in derivative pricing: the quasi-Monte Carlo (QMC) simulation which is an SDE-based approach (Glasserman 2013) and the finite-difference method which is a partial differential equation (PDE)-based approach (Duffy 2013). One usually uses the simulation approach for the qG model because it is often required to calculate the expectation of the stochastic process in several dimensions.

For models without volatility smile, it is not difficult to calculate the expectation since the exact discretization formulas of the relevant stochastic process are usually available. However, to fit the volatility smile better, one has to use models with a volatility smile such as the stochastic volatility model and the local volatility model. To implement the QMC simulation in these models, one cannot avoid discretizing the stochastic process with some approximation method, thus discretization errors are inevitable. Therefore, it is required to take a moderate number of partitions to reduce the error; as a result, the calculation costs become enormous. In fact, practitioners are struggling with the calculation cost to price exotic derivatives (e.g. Snowball, Target redemption note) in the qG models with volatility smiles. To overcome this problem, we consider reducing the number of partitions using the higher-order discretization methods of SDEs in this paper. Note that there have been some attempts to apply the higher-order discretization methods to practical problems (Andersen 2008, Alfonsi 2010, Ahdida *et al.* 2017), and practitioners usually use the conventional Euler–Maruyama (E–M) method (Maruyama 1955) or moment matching methods such as the quadratic-exponential (QE) method (Andersen 2008) to discretize the qG model.

1.1.3. Higher-order discretization method. Many studies have been conducted on higher-order discretization methods for SDEs; refer to monographs (Kloeden and Platen 1999, Glasserman 2013). Milstein proposed a higher-order method for SDEs driven by one-dimensional Brownian motion (Milstein 1975), and Talay and Tubaro proved the

applicability of Romberg extrapolation to the E–M method (Talay and Tubaro 1990).

In particular, Kusuoka (2001) introduced a new higher-order discretization framework called Kusuoka–Lyons–Ninomiya–Victoir scheme (KLVN-scheme) (Kusuoka 2013) that enables higher-order weak approximations for a very general class of SDEs driven by multi-dimensional Brownian motion. Since then, the KLVN-scheme has been developed in Ninomiya (2003), Kusuoka (2004), Lyons and Victoir (2004), Ninomiya and Victoir (2008) and Ninomiya and Ninomiya (2009). Using the framework of the KLVN-scheme, the Ninomiya–Victoir (N–V) (Ninomiya and Victoir 2008) and Ninomiya–Ninomiya (N–N) (Ninomiya and Ninomiya 2009) methods have been proposed as practically feasible second-order methods, and the $Q_{(s)}^{(7,2)}$ method (Shinozaki 2016, 2017) as a third-order method for an SDE driven by two-dimensional Brownian motion. When one executes simulation using these methods, it is required to solve a large number of ordinary differential equations (ODEs). It is evident, therefore, that the total calculation costs of these methods rely heavily on the ability to solve ODEs quickly and accurately. Although there are techniques to execute the simulation without solving ODEs numerically in some cases of the N–V and N–N schemes (Ninomiya and Victoir 2008, Bayer *et al.* 2013, Morimoto and Sasada 2017), one generally cannot avoid solving ODEs numerically.

In addition, extrapolation techniques enable us to increase the order of some discretization methods of SDE; it has been proved that an arbitrary high-order can be achieved by combining them with Romberg extrapolation (Kusuoka 2013) or Richardson extrapolation (Fujiwara 2006, Oshima *et al.* 2012). We also note that recent studies have attempted to apply the higher-order discretization methods to the computational challenge of forward-backward SDEs (Crisan and Manolarakis 2012, 2014, Ninomiya and Shinozaki 2019).

1.2. Results

In this paper, we present efficient simulation methods for the quasi-Gaussian term-structure model with stochastic volatility (qG-SV model) using the KLVN-scheme. We consider two types of stochastic volatility modeling: the Cox–Ingersoll–Ross (CIR) type (Cox *et al.* 1985) which is a principal method of stochastic volatility modeling and the Exponential Ornstein–Uhlenbeck (EXOU) type (Barndorff-Nielsen and Shephard 2001a, 2001b, Nicolato and Venardos 2003, Perelló *et al.* 2008). We demonstrate that our methods are even more efficient for the EXOU type compared with the case of CIR. Specifically, for the EXOU type model, the explicit discretizations (i.e. the explicit approximate or closed-form solutions of ODEs that are involved in executing the simulation) are constructed in all the N–V, N–N and $Q_{(s)}^{(7,2)}$ methods. In particular, to the best of our knowledge, there is no practical model with explicit third-order discretization. In fact, the nice algebraic properties of the vector fields of the qG-SV model enable us to apply the KLVN-scheme even effectively, thus resulting in the practical use of the KLVN-scheme.

Moreover, we present the numerical examples of a practically important problem: the pricing of Snowballs. The

Snowball is one of the major exotic derivative instruments, which has a strong path-dependence as coupons depend on all previous coupons. Numerical results show the effectiveness of the KLVN-scheme for these kinds of practical high-dimensional problems, especially when explicit discretizations are available, such as for the qGSV-EXOU model.

2. Previous studies of higher-order discretization methods of SDE

In this section, we introduce some notations and previous studies on higher-order discretization methods of SDE, especially on the KLVN-scheme, for later use.

2.1. Simulation approach

First, we formulate the weak approximation problem of SDEs. Let (Ω, \mathcal{F}, P) be a probability space and $(B^1(t), \dots, B^d(t))$ be a d -dimensional standard Brownian motion. $C_b^\infty(\mathbb{R}^N; \mathbb{R}^N)$ is the space of \mathbb{R}^N -valued smooth functions defined in \mathbb{R}^N whose derivatives of any order are bounded. Let $X : \Omega \times [0, \infty) \times \mathbb{R}^N \rightarrow \mathbb{R}^N$ be a solution of the SDE written in Stratonovich form as

$$\begin{aligned} X(t, x_0) = & x_0 + \int_0^t V_0(X(s, x_0)) ds \\ & + \sum_{i=1}^d \int_0^t V_i(X(s, x_0)) \circ dB^i(s), \end{aligned} \quad (1)$$

where $x_0 \in \mathbb{R}^N$, $V_0, V_1, \dots, V_d \in C_b^\infty(\mathbb{R}^N; \mathbb{R}^N)$. Here, $V \in C_b^\infty(\mathbb{R}^N; \mathbb{R}^N)$ can be identified as a smooth vector field on \mathbb{R}^N via $Vf(x) = \sum_{j=1}^N V^{(j)}(x)(\partial f / \partial x_j)(x)$ for $f \in C_b^\infty(\mathbb{R}^N; \mathbb{R})$, and SDE (1) can also be written in Ito form:

$$\begin{aligned} X(t, x_0) = & x_0 + \int_0^t \tilde{V}_0(X(s, x_0)) ds \\ & + \sum_{i=1}^d \int_0^t V_i(X(s, x_0)) dB^i(s), \end{aligned}$$

where $\tilde{V}_0^{(j)}(x) = V_0^{(j)}(x) + \frac{1}{2} \sum_{i=1}^d V_i V_i^{(j)}(x)$. In this paper, we call the numerical evaluation of $E[f(X(T, x_0))]$ as the weak approximation problem of SDEs. There are two approaches to solving this problem: performing simulations and using numerical methods for PDEs. As noted, we focus on the simulation approach in this paper.

In the simulation approach, the calculations are implemented in two steps. The first step is the discretization of SDEs, i.e. the construction of a set of random variables $\{\tilde{X}_{t_k, x_0}^{(n)}\}_{k=0,1,\dots,n}$ ($0 = t_0 < t_1 < \dots < t_n = T$) that approximates $\{X(t, x_0)\}_{0 \leq t \leq T}$. Here, n represents the number of partitions of $[0, T]$, and let $(\tilde{\Omega}, \tilde{\mathcal{F}}, \tilde{P})$ be a probability space on which these random variables are defined. The second step is the calculation of $\hat{E}[f(\tilde{X}_{T, x_0}^{(n)})]$ where \hat{E} denotes the expectation under \tilde{P} . The calculation involves the calculation of a finite-dimensional integration, and $D(n)$ denotes the number of dimensions of the integration. One usually calculates the integral using the Monte Carlo or quasi-Monte Carlo

method (Niederreiter 1992). Two types of approximation errors are involved in the calculations, namely, discretization and integration errors. The discretization error is the difference between $E[f(X(T, x_0))]$ and $\hat{E}[f(\tilde{X}_{T, x_0}^{(n)})]$, and an integration error is the error when one approximates the expectation \hat{E} with the sum of a random sample generated using the Monte Carlo method or the quasi-Monte Carlo method. When the discretization error is $O(p)$, i.e. when there exists a positive constant C_p such that

$$\left| E[f(X(T, x_0))] - \hat{E}\left[f\left(\tilde{X}_{T, x_0}^{(n)}\right)\right] \right| < C_p n^{-p},$$

it is said that the discretization method is of order p . Here, we define the order of the discretization method for weak approximation of SDEs; we discuss the order in this sense hereinafter.

The Euler–Maruyama (E–M) method (Maruyama 1955) is a well-known first-order discretization method for SDEs.

PROPOSITION 1 (First-order discretization method: Euler–Maruyama (Maruyama 1955, Talay and Tubaro 1990, Bally and Talay 1996)) The set of random variables $\{\tilde{X}_{t_k, x_0}^{(EM)}\}_{k=0,1,\dots,n}$ generated by the E–M is defined as follows:

$$\begin{aligned} \tilde{X}_{t_0, x_0}^{(EM)} &= x_0, \\ \tilde{X}_{t_{k+1}, x_0}^{(EM)} &= \tilde{X}_{t_k, x_0}^{(EM)} + \tilde{V}_0(\tilde{X}_{t_k, x_0}^{(EM)})s_k + \sum_{i=1}^d V_i(\tilde{X}_{t_k, x_0}^{(EM)})\eta_i^{(k+1)}\sqrt{s_k} \end{aligned}$$

where $\{\eta_i^{(k)}\}_{i=1,\dots,d, k=1,\dots,n}$ is a family of independent standard normal random variables and $s_k = t_{k+1} - t_k$. Then, under the appropriate nondegeneracy condition on V_0, V_1, \dots, V_d (Refer to Theorem 3.1 of Bally and Talay 1996), there exists a constant $C^{(EM)}$ such that

$$\left| E[f(X(T, x_0))] - \hat{E}\left[f\left(\tilde{X}_{T, x_0}^{(EM)}\right)\right] \right| < C^{(EM)} \frac{1}{n},$$

where $X(\cdot, x_0)$ is a solution to SDE (1) and $f : \mathbb{R}^N \rightarrow \mathbb{R}$ is a measurable and bounded function.

We can see that the number $D^{(EM)}(n)$ of dimensions of the integration $\hat{E}[f(\tilde{X}_{T, x_0}^{(EM)})]$ is $n \times d$.

2.2. KLVN-scheme

Then, we present the algorithms of the higher-order discretization methods that we use in this paper: the N–V, N–N, and $Q_{(s)}^{(7,2)}$ methods. As mentioned in Section 1, these methods are based on the framework of KLVN-scheme; refer to the original articles (Kusuoka 2001, 2003, 2004, Ninomiya and Victoir 2008, Ninomiya and Ninomiya 2009, Kusuoka 2013, Shinzaki 2017), for the theoretical details.

To present the algorithms of these methods, let us introduce the following notation. For a vector field $V \in C_b^\infty(\mathbb{R}^N; \mathbb{R}^N)$, $s \in [0, \infty)$, and $x \in \mathbb{R}^N$, $\exp(sV)(x)$ denotes the solution at time s of the ODE

$$\frac{dz(t)}{dt} = V(z(t)), \quad z(0) = x. \quad (2)$$

In other words, $\exp(sV) : \mathbb{R}^N \rightarrow \mathbb{R}^N$ is a diffeomorphism of the flow of V . In addition, for smooth vector fields $W_1, W_2 \in$

$C_b^\infty(\mathbb{R}^N; \mathbb{R}^N)$, we define the Lie bracket of vector fields as $[W_1, W_2] = W_1 W_2 - W_2 W_1$. It is well known that $[W_1, W_2]$ is also a smooth vector field on \mathbb{R}^N .

PROPOSITION 2 (Second-order discretization method: Ninomiya and Victoir 2008, Kusuoka 2013) Let $\{\eta_i^{(k)}\}_{i=1, \dots, d+1, k=1, \dots, n}$ be a family of independent standard normal random variables and $s_k = t_{k+1} - t_k$, the set of random variables $\{\tilde{X}_{t_k, x_0}^{(NV)}\}_{k=0, 1, \dots, n}$ generated by the Ninomiya–Victoir (N–V) method (Ninomiya and Victoir 2008) is defined as follows

$$\tilde{X}_{t_0, x_0}^{(NV)} = x_0,$$

$$\tilde{X}_{t_{k+1}, x_0}^{(NV)} = \begin{cases} \exp\left(\frac{s_k V_0}{2}\right) \circ \exp(\sqrt{s_k} \eta_1^{(k+1)} V_1) \cdots \\ \quad \circ \exp(\sqrt{s_k} \eta_d^{(k+1)} V_d) \circ \exp\left(\frac{s_k V_0}{2}\right) (\tilde{X}_{t_k, x_0}^{(NV)}) \\ \quad \text{if } \eta_{d+1}^{(k+1)} \geq 0, \\ \exp\left(d \frac{s_k V_0}{2}\right) \circ \exp(\sqrt{s_k} \eta_d^{(k+1)} V_d) \cdots \\ \quad \circ \exp(\sqrt{s_k} \eta_1^{(k+1)} V_1) \circ \exp\left(\frac{s_k V_0}{2}\right) (\tilde{X}_{t_k, x_0}^{(NV)}) \\ \quad \text{if } \eta_{d+1}^{(k+1)} < 0. \end{cases}$$

Then, under the UFG condition on V_0, V_1, \dots, V_d (refer to Kusuoka 2003), there exists a constant $C^{(NV)}$ which depends only on $\|f\|_{\text{Lip}}$, where $\|\cdot\|_{\text{Lip}}$ denotes the uniform norm, such that

$$|E[f(X(T, x_0))] - \hat{E}[f(\tilde{X}_{T, x_0}^{(NV)})]| < C^{(NV)} \frac{1}{n^2}.$$

PROPOSITION 3 (Second-order discretization method: Ninomiya and Ninomiya 2009, Kusuoka 2013) Let $\{\eta_i^{(k)}, \xi_i^{(k)}\}_{i=1, \dots, d, k=1, \dots, n}$ be a family of independent standard normal random variables, the set of random variables $\{\tilde{X}_{t_k, x_0}^{(NN)}\}_{k=0, 1, \dots, n}$ generated by the Ninomiya–Ninomiya (N–N) method (Ninomiya and Ninomiya 2009) is defined as follows:

$$\tilde{X}_{t_0, x_0}^{(NN)} = x_0,$$

$$\tilde{X}_{t_{k+1}, x_0}^{(NN)} = \exp\left(c_1 s_k V_0 + \sum_{i=1}^d \sqrt{R_{11} s_k} \eta_i^{(k+1)} V_i\right) \circ \exp\left(c_2 s_k V_0 + \sum_{i=1}^d \left(\frac{R_{12}}{\sqrt{R_{11}}} \eta_i^{(k+1)} + \sqrt{R_{22} - \frac{R_{12}^2}{R_{11}}} \xi_i^{(k+1)}\right) \sqrt{s_k} V_i\right) (\tilde{X}_{t_k, x_0}^{(NN)}), \quad (3)$$

where $c_1 = \frac{\pm\sqrt{2(2u-1)}}{2}$, $c_2 = 1 \pm \frac{\sqrt{2(2u-1)}}{2}$, $R_{11} = u$, $R_{22} = 1 + u \pm \sqrt{2(2u-1)}$, $R_{12} = -u \mp \frac{\sqrt{2(2u-1)}}{2}$ for some $u \geq 1/2$. Then, under the UFG condition on V_0, V_1, \dots, V_d , there exists a constant $C^{(NN)}$ which depends only on $\|f\|_{\text{Lip}}$ such that

$$|E[f(X(T, x_0))] - \hat{E}[f(\tilde{X}_{T, x_0}^{(NN)})]| < C^{(NN)} \frac{1}{n^2}.$$

Next, we present a third-order method for an SDE driven by two-dimensional Brownian motion.

PROPOSITION 4 (Third-order discretization method: $Q_{(s)}^{(7,2)}$ method Shinozaki 2017, Kusuoka 2001) Setting $d = 2$ and let $\{\eta_1^{(k)}, \eta_2^{(k)}, \eta_{12}^{(k)}, \eta_{01}^{(k)}, \eta_{02}^{(k)}, \eta_{112}^{(k)}, \eta_{122}^{(k)}\}_{k=1, \dots, n}$ be a family of independent standard normal random variables. The set of random variables by the $Q_{(s)}^{(7,2)}$ method $\{\tilde{X}_{t_k, x_0}^{(\text{third})}\}_{k=0, 1, \dots, n}$ is defined as follows:

$$\tilde{X}_{t_0, x_0}^{(\text{third})} = x_0,$$

$$\tilde{X}_{t_{k+1}, x_0}^{(\text{third})} = \exp\left(\left(\eta_1^{(k+1)} V_1 + \eta_2^{(k+1)} V_2\right) \sqrt{s_k} + \left(V_0 + \frac{\eta_{02}^{(k+1)} \eta_1^{(k+1)} + \eta_{01}^{(k+1)} \eta_2^{(k+1)} + \eta_{12}^{(k+1)}}{2\sqrt{3}} [V_1, V_2]\right) s_k + \left(\frac{-\eta_{01}^{(k+1)}}{2\sqrt{3}} [V_0, V_1] + \frac{\eta_{02}^{(k+1)}}{2\sqrt{3}} [V_0, V_2] + \frac{\eta_2^{(k+1)} + 2\eta_{112}^{(k+1)}}{12} [V_1, [V_1, V_2]] + \frac{\eta_1^{(k+1)} + 2\eta_{122}^{(k+1)}}{12} [[V_1, V_2], V_2]\right) s_k^{3/2} + \left(\frac{[[V_0, V_1], V_1]}{12} + \frac{[[V_0, V_2], V_2]}{12} + \frac{(\eta_{02}^{(k+1)} \eta_1^{(k+1)} + \eta_{01}^{(k+1)} \eta_2^{(k+1)} + \eta_{12}^{(k+1)})}{36\sqrt{3}} \times ([V_1, [V_1, [V_1, V_2]]] + [[V_1, V_2], V_2], V_2]\right) s_k^2 + \left(\frac{\eta_2^{(k+1)}}{360} [V_1, [V_1, [V_1, [V_1, V_2]]]] + \frac{\eta_1^{(k+1)}}{360} [V_1, [V_1, [[V_1, V_2], V_2]]] + \frac{\eta_1^{(k+1)}}{120} [[V_1, [V_1, V_2]], [V_1, V_2]] + \frac{\eta_2^{(k+1)}}{360} [V_1, [[[V_1, V_2], V_2], V_2]] + \frac{\eta_2^{(k+1)}}{90} [[V_1, V_2], [[V_1, V_2], V_2]] + \frac{\eta_1^{(k+1)}}{360} [[[[V_1, V_2], V_2], V_2], V_2]\right) s_k^{5/2} + \left(\frac{[[[[V_0, V_1], V_1], V_1], V_1]}{360} + \frac{[[[[V_0, V_2], V_2], V_2], V_2]}{360} + \frac{[V_0, [V_1, [[V_1, V_2], V_2]]]}{180} + \frac{[[V_0, [V_1, V_2]], [V_1, V_2]]}{60} + \frac{[[V_0, [[V_1, V_2], V_2]], V_1]}{120}\right) s_k^3$$

$$\begin{aligned}
& + \frac{[[V_0, V_2], [V_1, [V_1, V_2]]]}{120} \\
& + \frac{[[[V_0, V_2], [V_1, V_2]], V_1]}{90} \\
& + \frac{[[[[V_0, V_2], V_2], V_1], V_1]}{180} \Big) s_k^3 \Big) \left(\tilde{X}_{t_k, x_0}^{(\text{third})} \right). \quad (4)
\end{aligned}$$

Then, under the UFG condition on V_0, V_1, \dots, V_d , there exists a constant $C^{(\text{Third})}$ which depends only on $\|f\|_{\text{Lip}}$ such that

$$\left| E[f(X(T, x_0))] - \hat{E}\left[f\left(\tilde{X}_{T, x_0}^{(\text{Third})}\right)\right] \right| < C^{(\text{Third})} \frac{1}{n^3}.$$

REMARK 1 (Dimension of the $Q_{(s)}^{(7,2)}$ method) As described in Remark 3.7 in Shinozaki (2017), we can construct a third-order discretization method for arbitrary $d \geq 1$ by using the 7-moment similar family given in Theorem 3.1 of Shinozaki (2017), although we give the explicit construction of a third-order method only in the case of $d = 2$ to avoid presenting a complicated long formula due to the complexity of

$$\log \left(\sum_{\alpha \in A^*} s^{\frac{\|\alpha\|}{2}} Z_{\alpha} \alpha \right).$$

When applying to the qG models, we can obtain some simple explicit third-order methods by virtue of the algebraic structure of vector fields of the qG models; see remark 6.

REMARK 2 (Comparison of the N-V, N-N, $Q_{(s)}^{(7,2)}$ methods) We note that the numbers of dimensions of the integration are $D^{(\text{NV})}(n) = n \times (d + 1)$, $D^{(\text{NN})}(n) = n \times 2d$, and $D^{(\text{third})}(n) = n \times 7$ for the $Q_{(s)}^{(7,2)}$ method where $d = 2$. Hence, using higher-order discretization methods enables us to reduce n and thereby $D(n)$. Consequently, $E[f(X^{(n)}(T, x))]$ can be calculated through efficient use of the quasi-Monte Carlo method; see Remark 6.2 of Ninomiya and Ninomiya (2009).

In addition, the numbers $E(n)$ of ODEs to be solved are $E^{(\text{NV})}(n) = n \times (d + 2)$, $E^{(\text{NN})}(n) = n \times 2$, and $E^{(\text{third})}(n) = n \times 1$ for the $Q_{(s)}^{(7,2)}$ method where $d = 2$. Although the number of ODEs to be solved is increase as the dimension d of SDE increases in the N-V method, the involved ODEs are simpler and have closed-form solutions in some cases, which is a very nice property in the practical use. Furthermore, it is empirically known that $C^{(\text{EM})} \gg C^{(\text{NV})} > C^{(\text{NN})} \gg C^{(\text{Third})}$ holds; see, for example, the numerical experiments of Shinozaki (2017).

REMARK 3 (The regularity assumption on f) In the initial work of Kusuoka (2001, 2004), the estimations of discretization errors in proposition 2, 3, 4 are proved on the assumption of $f \in C_b^\infty(\mathbb{R}^N; \mathbb{R})$. It is easily seen that this assumption can be relaxed to $f \in C_{\text{Lip}}(\mathbb{R}^N; \mathbb{R})$, as pointed out in Section 3 of Lyons and Victoir (2004). Furthermore, for the N-V and N-N methods, it is proved that the condition on f can be relaxed to be a measurable and bounded function in Kusuoka (2013).

3. Discretization methods of the quasi-Gaussian term-structure models with stochastic volatility

In this section, the formulas for applying the KLVN-scheme to the qG-SV model are presented, which is the main contribution of this paper.

3.1. Quasi-Gaussian term-structure models with stochastic volatilities

Following the formulation in Section 13.3 of Anderson and Piterbarg (2010), we formulate the qG model as below. Let (Ω, \mathcal{F}, P) be a probability space and the filtration \mathcal{F}_t generated by the l -dimensional Brownian motion. Let the forward rate process $f(t, T)$ as

$$\begin{aligned}
f(t, T) = & f(t_0, T) + \int_{t_0}^t \int_s^T \sum_{i=1}^l \left(\sigma_f^{(i)}(s, u, \omega) \right)^2 du ds \\
& + \sum_{i=1}^l \int_0^t \sigma_f^{(i)}(s, T, \omega) dB_s^{(i)},
\end{aligned}$$

and $\sigma_f(s, T, \omega) := (\sigma_f^{(1)}(s, T, \omega), \dots, \sigma_f^{(l)}(s, T, \omega)) \in \mathbb{R}^l$. Then, we impose a separability condition on the volatility structure of the multi-factor HJM model;

$$\sigma_f(s, T, \omega) = g(s, \omega)h(T)$$

where $g : [0, \infty) \times \Omega \rightarrow \mathbb{R}^{l \times l}$ is an $l \times l$ matrix-valued \mathcal{F}_t -measurable stochastic process and $h : [0, \infty) \rightarrow \mathbb{R}^l$ is an l -dimensional vector-valued deterministic function. Let us further assume that $h^{(i)}(t) \neq 0$ for all $t > 0$, $i = 1, \dots, l$ and $H(t) := \text{diag}(h^{(1)}(t), \dots, h^{(l)}(t))$, where $h(t) = (h^{(1)}(t), \dots, h^{(l)}(t))$. Note that this separability condition enables us to represent the bond price $P(t, T)$ simply as later described in proposition 5. Setting $\sigma_r(t, \omega) := \sigma_f(t, t, \omega)$, we consider the solution $x(t) \in \mathbb{R}^l, y(t) \in \mathbb{R}^{l \times l}$ to the following SDEs (the qG model):

$$\begin{aligned}
dx(t) &= (y(t)\mathbf{1} - \kappa(t)x(t))dt + \sigma_r(t, \omega)dB(t), \\
dy(t) &= (\sigma_r(t, \omega)^t \sigma_r(t, \omega) - \kappa(t)y(t) - y(t)\kappa(t))dt, \\
x^{(i)}(0) &= y^{(ij)}(0) = 0, \text{ for } i, j = 1, \dots, l
\end{aligned}$$

where $B(t) = (B^{(1)}(t), \dots, B^{(l)}(t))$ is the l -dimensional Brownian motion and $dB(t)$ denotes the Ito form integral, $\sigma_r(t, \omega) \in \mathbb{R}^l, \kappa(t) \in \mathbb{R}^{l \times l}$. Then, the dynamics of $\{P(t, T)\}_{t_0 < t < T}$ can be described as follows.

PROPOSITION 5 (Bond reconstruction formula; Proposition 13.3.1 of Anderson and Piterbarg 2010)

$$\begin{aligned}
P(t, T) &= \frac{P(t_0, T)}{P(t_0, t)} \exp \left(-\int_{t_0}^t G(s, T)x(s)ds - \frac{1}{2} \int_{t_0}^t G(s, T)y(s)G(s, T)ds \right), \quad (5)
\end{aligned}$$

where $G(t, T) = \int_t^T H(s)H(s)^{-1}I ds$ is an l -dimensional vector and $I = (1, \dots, 1) \in \mathbb{R}^l$.

Note that $P(t, T)$ is a function of $x(t), y(t)$ and an \mathcal{F}_t -measurable random variable. Let $L(T_i, T_{i+1})$ denotes the interest rate (e.g. LIBOR) at time T_i for the period $[T_i, T_{i+1}]$ and assume that the fixing lag is zero for simplicity. As is well known, $L(T_i, T_{i+1})$ can be represented as a function of $B(T_i, T_{i+1})$, i.e.

$$L(T_i, T_{i+1}) = \frac{1}{\delta(T_i, T_{i+1})} \left(\frac{1}{P(T_i, T_{i+1})} - 1 \right), \quad (6)$$

where $\delta(T_{i-1}, T_i)$ is the day count of the period $[T_{i-1}, T_i]$. Thus, $L(T_i, T_{i+1})$ is also a function of $x(T_i), y(T_i)$ and an \mathcal{F}_{T_i} -measurable random variable. We can consequently formulate the prices of exotic interest rate derivatives, that are options on $\{L(T_i, T_{i+1})\}_{i=0,1,\dots,K-1}$, as an expectation of a function of $\{x(T_i), y(T_i)\}_{i=0,1,\dots,K-1}$. Therefore, we focus on the discretization of the process $x(t), y(t)$ subsequently in this paper.

Specifying $g(\cdot, \omega)$, we consider the following two types of quasi-Gaussian term-structure models with stochastic volatility (qG-SV model):

qGSV-CIR

$$\begin{aligned} dx(t) &= (y(t)\mathbf{1} - \kappa(t)x(t))dt + \sqrt{z(t)}\sigma(t)dB(t), \\ dy(t) &= (z(t)\sigma(t)' \sigma(t) - \kappa(t)y(t) - y(t)\kappa(t))dt, \\ dz(t) &= \theta(\xi - z(t))dt + \chi(t)\sqrt{z(t)}dZ(t), \\ \langle dB^{(i)}(t), dZ(t) \rangle &= \rho_i dt, \\ x^{(i)}(0) &= y^{(ij)}(0) = 0, \text{ for } i, j = 1, \dots, l, \text{ and } z(0) = z_0, \end{aligned} \quad (7)$$

qGSV-EXOU

$$\begin{aligned} dx(t) &= (y(t)\mathbf{1} - \kappa(t)x(t))dt + e^{w(t)}\sigma(t)dB(t), \\ dy(t) &= (e^{2w(t)}\sigma(t)' \sigma(t) - \kappa(t)y(t) - y(t)\kappa(t))dt, \\ dw(t) &= \theta(\xi - w(t))dt + \chi(t)dZ(t), \\ \langle dB^{(i)}(t), dZ(t) \rangle &= \rho_i dt, \\ x^{(i)}(0) &= y^{(ij)}(0) = 0, \text{ for } i, j = 1, \dots, l, \text{ and } w(0) = w_0, \end{aligned} \quad (8)$$

where $x(t), \sigma(t) \in \mathbb{R}^l, y(t), \kappa(t) \in \mathbb{R}^{l \times l}, z(t), w(t), \theta, \xi, \chi(t) \in \mathbb{R}$, and $\rho = (\rho_1, \dots, \rho_l) \in [0, 1]^l$. Here, $(B^{(1)}(t), \dots, B^{(l)}(t), Z(t))$ is the $(l+1)$ -dimensional Brownian motion, $B(t)$ denotes $(B^{(1)}(t), \dots, B^{(l)}(t))$, and $dB(t), dZ(t)$ denote the Ito form integrals. We call model (7) as quasi-Gaussian term-structure model with CIR-type stochastic volatility (qGSV-CIR), and model (8) as quasi-Gaussian term-structure model with exponential Ornstein–Uhlenbeck-type stochastic volatility (qGSV-EXOU) hereinafter. In this paper, we basically consider the case of $l = 1$ to avoid tedious complications; the extension to general $l > 0$ is not difficult in many cases, see remark 5, 6. In addition, we assume that $\kappa(t), \sigma(t), \chi(t)$ are constants for simplicity; thus we denote $\kappa, \sigma, \chi \in \mathbb{R}$ in (7), (8).

3.2. Vector fields of qG-SV model

The qGSV-CIR model (7) with $l = 1$ can be represented as $X(t, x_0)$ using the notation of the previous section as follows.

qGSV-CIR with $l=1$

$$\begin{aligned} X(t, x_0) &= x_0 + \int_0^t V_0^{\text{CIR}}(X(s, x_0))ds \\ &\quad + \sum_{i=1}^2 \int_0^t V_i^{\text{CIR}}(X(s, x_0)) \circ dB^i(s), \end{aligned}$$

where

$$\begin{aligned} V_0^{\text{CIR}} \begin{pmatrix} w_1 \\ w_2 \\ w_3 \end{pmatrix} &= \begin{pmatrix} w_2 - \kappa w_1 - \frac{\rho \chi \sigma}{4} \\ \sigma^2 w_3 - 2\kappa w_2 \\ \theta(\xi - w_3) - \frac{\chi^2}{4} \end{pmatrix}, \\ V_1^{\text{CIR}} \begin{pmatrix} w_1 \\ w_2 \\ w_3 \end{pmatrix} &= \begin{pmatrix} \sigma \sqrt{w_3} \\ 0 \\ \rho \chi \sqrt{w_3} \end{pmatrix}, \\ V_2^{\text{CIR}} \begin{pmatrix} w_1 \\ w_2 \\ w_3 \end{pmatrix} &= \begin{pmatrix} 0 \\ 0 \\ \sqrt{1 - \rho^2} \chi \sqrt{w_3} \end{pmatrix}. \end{aligned}$$

In the vector field form, $V_0^{\text{CIR}}, V_1^{\text{CIR}}, V_2^{\text{CIR}}$ can be represented as

$$\begin{aligned} V_0^{\text{CIR}} &= \left(w_2 - \kappa w_1 - \frac{\rho \chi \sigma}{4} \right) \frac{\partial}{\partial w_1} + (\sigma^2 w_3 - 2\kappa w_2) \frac{\partial}{\partial w_2} \\ &\quad + \left(\theta(\xi - w_3) - \frac{\chi^2}{4} \right) \frac{\partial}{\partial w_3}, \\ V_1^{\text{CIR}} &= \sigma \sqrt{w_3} \frac{\partial}{\partial w_1} + \rho \chi \sqrt{w_3} \frac{\partial}{\partial w_3}, \\ V_2^{\text{CIR}} &= \sqrt{1 - \rho^2} \chi \sqrt{w_3} \frac{\partial}{\partial w_3} \end{aligned}$$

On the other hand, the qGSV-EXOU model (8) can be written as follows.

$$\begin{aligned} X(t, x_0) &= x_0 + \int_0^t V_0^{\text{EXOU}}(X(s, x_0))ds \\ &\quad + \sum_{i=1}^2 \int_0^t V_i^{\text{EXOU}}(X(s, x_0)) \circ dB^i(s), \end{aligned}$$

where

$$\begin{aligned} V_0^{\text{EXOU}} \begin{pmatrix} w_1 \\ w_2 \\ w_3 \end{pmatrix} &= \begin{pmatrix} w_2 - \kappa w_1 - \frac{\rho \chi \sigma}{2} \exp(w_3) \\ \sigma^2 \exp(2w_3) - 2\kappa w_2 \\ \theta(\xi - w_3) \end{pmatrix}, \\ V_1^{\text{EXOU}} \begin{pmatrix} w_1 \\ w_2 \\ w_3 \end{pmatrix} &= \begin{pmatrix} \sigma \exp(w_3) \\ 0 \\ \rho \chi \end{pmatrix}, \\ V_2^{\text{EXOU}} \begin{pmatrix} w_1 \\ w_2 \\ w_3 \end{pmatrix} &= \begin{pmatrix} 0 \\ 0 \\ \sqrt{1 - \rho^2} \chi \end{pmatrix}. \end{aligned}$$

$V_0^{\text{EXOU}}, V_1^{\text{EXOU}}, V_2^{\text{EXOU}}$ can also be represented in the vector field form in the same way as the qGSV-CIR model.

3.3. Discretization formulas

In this section, the involved ordinary differential equations and some explicit discretization formulas of the N–V, N–N,

and $Q_{(s)}^{(7,2)}$ methods are presented. As discussed, the total simulation costs using these methods rely heavily on the ability to solve ODEs quickly and accurately. We can find the closed-form or approximate solutions in some cases; specifically, the N-V method for both the qGSV-CIR and qGSV-EXOU models, the N-N and $Q_{(s)}^{(7,2)}$ methods for the qGSV-EXOU model as described below. Using the following explicit formulas, one can easily implement higher-order discretization methods.

3.3.1. Ninomiya-Victoir method. In the N-V method, the involved ODEs are obvious from (2), therefore we omit. The closed-form solution for the qGSV-CIR model is as follows:

$$\begin{aligned} & \exp(sV_0^{\text{CIR}}) \begin{pmatrix} w_1 \\ w_2 \\ w_3 \end{pmatrix} \\ &= \begin{pmatrix} w_1 + \frac{\sigma^2(w_3 + J)}{(2\kappa - \theta)(\kappa - \theta)} (\exp(-\theta s) - \exp(-\kappa s)) \\ -\frac{\sigma^2}{\kappa} \left(\frac{J}{2\kappa} - \frac{w_3 + J}{2\kappa - \theta} \right) (\exp(-2\kappa s) \\ - \exp(-\kappa s)) + \frac{1}{\kappa} \left(w_2 - \frac{\sigma^2 J}{2\kappa} - \frac{\rho \chi \sigma}{4} \right) \\ \times (1 - \exp(-\kappa s)) \\ w_2 + \sigma^2 \left(\frac{w_3 + J}{2\kappa - \theta} (\exp(-\theta s) - \exp(-2\kappa s)) \right. \\ \left. - \frac{J}{2\kappa} (1 - \exp(-2\kappa s)) \right) \\ (w_3 + J) \exp(-\theta s) - J \end{pmatrix}, \\ & \exp(sV_1^{\text{CIR}}) \begin{pmatrix} w_1 \\ w_2 \\ w_3 \end{pmatrix} = \begin{pmatrix} \left(\frac{\sigma}{2} s + \sqrt{w_3} \right)^2 \\ w_2 \\ \left(\frac{\rho \chi}{2} s + \sqrt{w_3} \right)^2 \end{pmatrix}, \\ & \exp(sV_2^{\text{CIR}}) \begin{pmatrix} w_1 \\ w_2 \\ w_3 \end{pmatrix} = \begin{pmatrix} w_1 \\ w_2 \\ \left(\frac{\sqrt{1 - \rho^2} \chi}{2} s + \sqrt{w_3} \right)^2 \end{pmatrix}, \quad (9) \end{aligned}$$

where $J := \xi - \frac{\chi^2}{4\theta}$. On the other hand, an approximate solution for the qGSV-EXOU model is as follows:

$$\begin{aligned} & \exp(sV_0^{\text{EXOU}}) \begin{pmatrix} w_1 \\ w_2 \\ w_3 \end{pmatrix} \\ &= \begin{pmatrix} \left(w_1 + \left(w_2 - \frac{\sigma^2 \exp(2w_3)}{A} \right) \frac{1 - \exp(-\kappa s)}{\kappa} \right. \\ + \frac{\sigma^2 \exp(2w_3)}{A(A - \kappa)} (\exp((A - \kappa)s) - 1) \\ - \frac{\chi \rho \sigma \exp(w_3)}{A} \left(\exp\left(\frac{As}{2}\right) - 1 \right) + \mathcal{O}(s^3) \\ \times \exp(-\kappa s) \\ \left(w_2 + \sigma^2 \exp(2w_3) \left(\frac{\exp(sA) - 1}{A} + \mathcal{O}(s^3) \right) \right) \\ \times \exp(-2\kappa s) \\ \xi - (\xi - w_3) \exp(-\theta s) \end{pmatrix}, \end{aligned}$$

$$\begin{aligned} & \exp(sV_1^{\text{EXOU}}) \begin{pmatrix} w_1 \\ w_2 \\ w_3 \end{pmatrix} \\ &= \begin{pmatrix} w_1 + \frac{\sigma \exp(w_3) (\exp(\chi \rho s) - 1)}{\chi \rho} \\ w_2 \\ w_3 + \chi \rho s \end{pmatrix}, \\ & \exp(sV_2^{\text{CIR}}) \begin{pmatrix} w_1 \\ w_2 \\ w_3 \end{pmatrix} = \begin{pmatrix} w_1 \\ w_2 \\ w_3 + \chi \sqrt{1 - \rho^2} s \end{pmatrix}, \end{aligned}$$

where $A = 2(\kappa + (\xi - w_3)\theta)$.

REMARK 4 (Derivation of approximate solutions of ODEs) In this section, several approximate solutions of ODEs are derived by virtue of the Taylor expansion.

For example, an approximate solution to $\exp(sV_0^{\text{EXOU}})(w_1, w_2, w_3)$ is derived as follows. $\exp(sV_0^{\text{EXOU}})(w_1, w_2, w_3)$ is the solution at time s of the ODEs

$$\begin{aligned} \frac{dv_1(t)}{dt} &= v_2(t) - \kappa v_1(t) - \frac{\rho \chi \sigma}{2} \exp(v_3(t)) \\ \frac{dv_2(t)}{dt} &= \sigma^2 \exp(2v_3(t)) - 2\kappa v_2(t) \\ \frac{dv_3(t)}{dt} &= \theta(\xi - v_3(t)) \end{aligned}$$

with the initial condition $v_1(0) = w_1, v_2(0) = w_2, v_3(0) = w_3$. It is easy to find the closed-form solution to the third coordinate $v_3(t) = \xi - (\xi - w_3) \exp(-\theta t)$. Next, to construct an approximate solution to the second coordinate, we set $v_2(t) = g(t) \exp(-2\kappa t)$. Then, $g(t)$ satisfies the following ODE

$$\frac{dg(t)}{dt} = \sigma^2 \exp(2v_3(t) + 2\kappa t), \quad g(0) = w_2. \quad (10)$$

An approximate solution to the ODE (10) can be constructed as follows.

$$\begin{aligned} g(t) &= w_2 + \int_0^t \sigma^2 \exp(2v_3(u) + 2\kappa u) du \\ &= w_2 + \int_0^t \sigma^2 \exp(2\xi - 2(\xi - w_3) \exp(-\theta u) + 2\kappa u) du \\ &= w_2 + \int_0^t \sigma^2 \exp(2\xi - 2(\xi - w_3) (1 - \theta u + \mathcal{O}(u^2)) \\ &\quad + 2\kappa u) du \\ &= w_2 + \sigma^2 \exp(2w_3) \int_0^t \exp(Au + \mathcal{O}(u^2)) du \\ &= w_2 + \sigma^2 \exp(2w_3) \left(\int_0^t \exp(Au) du + \mathcal{O}(t^3) \right) \\ &= w_2 + \sigma^2 \exp(2w_3) \left(\frac{\exp(tA) - 1}{A} + \mathcal{O}(t^3) \right) \end{aligned}$$

where $A = 2(\kappa + (\xi - w_3)\theta)$. Thus, we derive the approximate solution

$$\begin{aligned} v_2(t) &= \left(w_2 + \sigma^2 \exp(2w_3) \left(\frac{\exp(tA) - 1}{A} + \mathcal{O}(t^3) \right) \right) \\ &\quad \times \exp(-2\kappa t) \end{aligned}$$

The approximate solution to $v_1(t)$ can be constructed in a similar way. Setting $v_1(t) = h(t) \exp(-\kappa t)$, an approximate solution to $h(t)$ can be constructed as follows.

$$\begin{aligned}
 h(t) &= w_1 + \int_0^t \exp(\kappa u) \left(v_2(u) - \frac{\rho \chi \sigma}{2} \exp(v_3(u)) \right) du \\
 &= w_1 + \int_0^t \exp(\kappa u) \left(\left(w_2 + \sigma^2 \exp(2w_3) \right) \right. \\
 &\quad \times \left(\frac{\exp(uA) - 1}{A} + \mathcal{O}(u^3) \right) \exp(-2\kappa u) \\
 &\quad \left. - \frac{\rho \chi \sigma}{2} \exp(\xi - (\xi - w_3) \exp(-\theta u)) \right) du \\
 &= w_1 + \int_0^t \left(\left(w_2 - \frac{\sigma^2 \exp(2w_3)}{A} \right) \exp(-\kappa u) \right. \\
 &\quad \left. + \frac{\sigma^2 \exp(2w_3)}{A} \exp((A - \kappa)u) + \mathcal{O}(u^3) - \frac{\rho \chi \sigma}{2} \right. \\
 &\quad \left. \times \exp(\kappa u + \xi - (\xi - w_3)(1 - \theta u + \mathcal{O}(u^2))) \right) du \\
 &= w_1 + \int_0^t \left(w_2 - \frac{\sigma^2 \exp(2w_3)}{A} \right) \exp(-\kappa u) \\
 &\quad + \frac{\sigma^2 \exp(2w_3)}{A} \exp((A - \kappa)u) \\
 &\quad - \frac{\rho \chi \sigma}{2} \exp\left(w_3 + \frac{A}{2}u\right) + \mathcal{O}(u^2) du \\
 &= w_1 + \left(w_2 - \frac{\sigma^2 \exp(2w_3)}{A} \right) \frac{1 - \exp(-\kappa t)}{\kappa} \\
 &\quad + \frac{\sigma^2 \exp(2w_3)}{A(A - \kappa)} (\exp((A - \kappa)t) - 1) \\
 &\quad - \frac{\chi \rho \sigma \exp(w_3)}{A} \left(\exp\left(\frac{At}{2}\right) - 1 \right) + \mathcal{O}(t^3)
 \end{aligned}$$

REMARK 5 (Extension to the general $l > 0$ case) In the general $l > 0$ case, the qGSV-CIR model (7) can be represented as $X(t, x_0)$ using the notation of the previous section as follows.

$$\begin{aligned}
 X(t, x_0) &= x_0 + \int_0^t V_0^{\text{CIR}}(X(s, x_0)) ds \\
 &\quad + \sum_{i=1}^{l+1} \int_0^t V_i^{\text{CIR}}(X(s, x_0)) \circ dB^i(s),
 \end{aligned}$$

where

$$\begin{aligned}
 V_0^{\text{CIR}} &= \sum_{k=1}^l \left(\sum_{j=1}^l y^{(1j)} - \kappa_i x^{(k)} - \frac{\rho_k \sigma_k \chi}{4} \right) \frac{\partial}{\partial x^{(k)}} \\
 &\quad + \sum_{k=1}^l (\sigma_k^2 z - 2\kappa_k y^{(kk)}) \frac{\partial}{\partial y^{(kk)}} \\
 &\quad - \sum_{1 \leq j < k \leq l} (\kappa_j + \kappa_k) y^{(jk)} \frac{\partial}{\partial y^{(jk)}} + \left(\theta(\xi - z) - \frac{\chi^2}{4} \right) \frac{\partial}{\partial z}, \\
 V_i^{\text{CIR}} &= \sigma_i \sqrt{z} \frac{\partial}{\partial x^{(i)}} + \rho_i \chi \sqrt{z} \frac{\partial}{\partial z} \quad (i = 1, \dots, l+1),
 \end{aligned}$$

$$\text{and } \sigma_{l+1} = 0, \rho_{l+1} + \sqrt{1 - \sum_{i=1}^l \rho_i^2}.$$

It is easily seen that $\exp(sV_0^{\text{CIR}}), \exp(sV_1^{\text{CIR}}), \dots, \exp(sV_{l+1}^{\text{CIR}})$ can be represented as the closed-form solutions in similar manner to the case of $l = 1$. Thus, we can apply the N–V method for the general $l > 0$ case. Note that we can extend to the general $l > 0$ case also in the qGSV-EXOU model.

3.3.2. Ninomiya–Ninomiya method. In the N–N method, one can find a closed-form solution for the qGSV-CIR model using special functions; however, this closed-form solution is inappropriate in practical use due to the difficulty of computing the special functions. Therefore, we apply the Runge–Kutta (R–K) method to solve ODEs (11) in the numerical experience of the next section. In the qGSV-CIR model, we obtain the ODEs to be solved in the N–N method by substituting the vector field in (3) as follows.

$$\begin{aligned}
 &\exp \left(c_1 s_k V_0^{\text{CIR}} + \sum_{i=1}^2 \sqrt{R_{11} s_k} \eta_i^{(k)} V_i^{\text{CIR}} \right) \begin{pmatrix} w_1 \\ w_2 \\ w_3 \end{pmatrix} \\
 &= \exp \left(\left(c_1 s_k \left(w_2 - \kappa w_1 - \frac{\rho \chi \sigma}{4} \right) \right. \right. \\
 &\quad \left. \left. + \sqrt{R_{11} s_k} \eta_1^{(k)} (\sigma \sqrt{w_3}) \right) \frac{\partial}{\partial w_1} + c_1 s_k (\sigma^2 w_3 - 2\kappa w_2) \frac{\partial}{\partial w_2} \right. \\
 &\quad \left. + \left(c_1 s_k \left(\theta(\xi - w_3) - \frac{\chi^2}{4} \right) + \sqrt{R_{11} s_k} (\eta_1^{(k)} (\rho \chi \sqrt{w_3}) \right. \right. \right. \\
 &\quad \left. \left. \left. + \eta_2^{(k)} (\sqrt{1 - \rho^2 \chi} \sqrt{w_3}) \right) \right) \frac{\partial}{\partial w_3} \right) \begin{pmatrix} w_1 \\ w_2 \\ w_3 \end{pmatrix}.
 \end{aligned}$$

Hence, $\exp(c_1 s_k V_0^{\text{CIR}} + \sum_{i=1}^2 \sqrt{R_{11} s_k} \eta_i^{(k)} V_i^{\text{CIR}})(t(w_1, w_2, w_3))$ is the value at $t = 1$ of a solution $(v_1(t), v_2(t), v_3(t))$ to the following ODEs:

$$\begin{aligned}
 \frac{d}{dt} v_1(t) &= c_1 s_k \left(v_2(t) - \kappa v_1(t) - \frac{\rho \chi \sigma}{4} \right) \\
 &\quad + \sqrt{R_{11} s_k} \eta_1^{(k)} \sigma \sqrt{v_3(t)}, \\
 \frac{d}{dt} v_2(t) &= c_1 s_k (\sigma^2 v_3(t) - 2\kappa v_2(t)), \\
 \frac{d}{dt} v_3(t) &= c_1 s_k \left(\theta(\xi - v_3(t)) - \frac{\chi^2}{4} \right) \\
 &\quad + \sqrt{R_{11} s_k} \left(\eta_1^{(k)} \rho \chi + \eta_2^{(k)} \sqrt{1 - \rho^2 \chi} \right) \sqrt{v_3(t)},
 \end{aligned} \tag{11}$$

with the initial condition $v_1(0) = w_1, v_2(0) = w_2, v_3(0) = w_3$. For the other exponential $\exp(c_2 s_k V_0^{\text{CIR}} + \sum_{i=1}^2 (\frac{R_{12}}{\sqrt{R_{11}}} \eta_i^{(k+1)} + \sqrt{R_{22} - \frac{R_{12}^2}{R_{11}}} \xi_i^{(k+1)}) \sqrt{s_k} V_i^{\text{CIR}})$, the ODEs to be solved can be derived in the same way, so we omit them.

For the qGSV-EXOU model, we can derive the ODEs also in the same way. An approximate solution of the ODEs is as follows:

$$\exp \left(a_0 s_k V_0^{\text{EXOU}} + \sum_{i=1}^2 a_i \sqrt{s_k} \eta_i^{(k)} V_i^{\text{EXOU}} \right) \begin{pmatrix} w_1 \\ w_2 \\ w_3 \end{pmatrix}$$

$$= \begin{pmatrix} e^{-\kappa a_0 s_k} \left(w_1 + \frac{w_2(1 - e^{-\kappa a_0 s_k})}{\kappa} + a_0^2 s_k^2 \sigma^2 e^{2w_3} \right. \\ \times \left(\frac{1}{2} + \frac{\alpha_1 - \kappa a_0 s_k}{3} + \frac{\alpha_2 + 2\alpha_1^2}{12} - \frac{\alpha_1 \kappa a_0 s_k}{4} \right. \\ \left. \left. + \frac{\kappa^2 a_0^2 s_k^2}{8} \right) + \left(-\frac{a_0 s_k \rho \chi \sigma}{2} + a_1 \sqrt{s_k} \sigma \right) e^{w_3} \right. \\ \left. \left(1 + \frac{\alpha_1}{2} + \frac{\alpha_2 + \alpha_1^2}{6} + \frac{\alpha_3}{24} + \frac{\alpha_1 \alpha_2}{16} + \frac{\alpha_1^3}{24} \right) \right) \\ + \mathcal{O}(s_k^3) \\ e^{-2\kappa a_0 s_k} \left(w_2 + a_0 s_k \sigma^2 e^{2w_3} \left(1 + \alpha_1 + \frac{\alpha_2 + 2\alpha_1^2}{3} \right. \right. \\ \left. \left. + \frac{\alpha_3}{12} + \frac{\alpha_1 \alpha_2}{2} + \frac{\alpha_1^3}{3} \right) \right) + \mathcal{O}(s_k^3) \\ \left. e^{-a_0 s_k \theta} \left(w_3 + \frac{b_1(e^{a_0 s_k \theta} - 1)}{a_0 s_k \theta} \right) \right) \end{pmatrix},$$

where $b_1 = a_0 s_k \theta \xi + a_1 \sqrt{s_k} \chi \rho \eta_1^{(k)} + a_2 \sqrt{s_k} \chi \sqrt{1 - \rho^2} \eta_2^{(k)}$, $\alpha_1 = b_1 - a_0 s_k \theta w_3 + \kappa a_0 s_k$, $\alpha_2 = a_0^2 s_k^2 \theta^2 w_3 - a_0 s_k \theta b_1$, $\alpha_3 = a_0^2 s_k^2 \theta^2 b_1 - a_0^3 s_k^3 \theta^2 w_3$. Substituting $a_0 = c_1$, $a_1 = \sqrt{R_{11}} \eta_1^{(k+1)}$, $a_2 = \sqrt{R_{11}} \eta_2^{(k+1)}$ and $a_0 = c_2$, $a_1 = \frac{R_{12}}{\sqrt{R_{11}}} \eta_1^{(k+1)} + \sqrt{R_{22} - \frac{R_{12}^2}{R_{11}}}$, $\xi_1^{(k+1)}$, $a_2 = \frac{R_{12}}{\sqrt{R_{11}}} \eta_2^{(k+1)} + \sqrt{R_{22} - \frac{R_{12}^2}{R_{11}} \xi_2^{(k+1)}}$, we thus obtain an approximate solution in the N-N method for the qGSV-EXOU model.

3.3.3. $\mathcal{Q}_{(s)}^{(7,2)}$ method. First, to implement $\mathcal{Q}_{(s)}^{(7,2)}$ method for the qGSV-CIR model, the following algebraic structure of V_1^{CIR} is noteworthy: $[V_1^{\text{CIR}}, V_2^{\text{CIR}}]$ is a constant, i.e.

$$[V_1^{\text{CIR}}, V_2^{\text{CIR}}] = -\frac{\sigma \chi \sqrt{1 - \rho^2}}{2} \frac{\partial}{\partial w_3}. \quad (12)$$

This algebraic structure drastically simplify the third-order method; in fact, many terms in (4) equal to zero. Thus the ODEs to be solved in the $\mathcal{Q}_{(s)}^{(7,2)}$ method is simpler compared to other cases, although we cannot find closed-form or approximate solution without special functions. We apply the R-K method to solve the ODEs (13) in the numerical experience of the next section. $\tilde{X}_{t_{k+1}, x_0}^{(\text{third}, \text{CIR})}$ is the value at $t = 1$ of a solution $(v_1(t), v_2(t), e^{v_3(t)})$ to the following ODEs:

$$\begin{aligned} \frac{d}{dt} v_1(t) &= \sigma \eta_1^{(k+1)} e^{\frac{v_3(t)}{2}} \sqrt{s_k} \\ &+ \left(v_2(t) - \kappa v_1(t) - \frac{\rho \chi \sigma}{4} \right. \\ &\left. - \frac{\sigma I (\eta_{02}^{(k+1)} \eta_1^{(k+1)} + \eta_{01}^{(k+1)} \eta_2^{(k+1)} + \eta_{12}^{(k+1)})}{4\sqrt{3}} \right) s_k \\ &+ \left(\frac{\theta \sigma \eta_{01}^{(k+1)}}{4\sqrt{3}} \left(e^{\frac{v_3(t)}{2}} - J e^{-\frac{v_3(t)}{2}} \right) - \frac{\eta_{01}^{(k+1)} \kappa \sigma}{2\sqrt{3}} e^{\frac{v_3(t)}{2}} \right) s_k^{\frac{3}{2}} \\ &+ \frac{\rho \chi \sigma (\theta (1 + J e^{-v_3(t)}) - \kappa)}{24} s_k^2 + \frac{\theta \sigma \chi^3 J e^{-2v_3(t)}}{240} s_k^3, \\ \frac{d}{dt} v_2(t) &= (e^{v_3(t)} \sigma^2 - 2\kappa v_2(t)) s_k \end{aligned}$$

$$\begin{aligned} &+ \frac{\sigma^2 (\rho \chi \eta_{01}^{(k+1)} - I \eta_{02}^{(k+1)}) e^{\frac{v_3(t)}{2}}}{2\sqrt{3}} s_k^{\frac{3}{2}} + \frac{\sigma^2 \chi^2}{24} s_k^2, \\ \frac{d}{dt} v_3(t) &= (\rho \chi \eta_1^{(k+1)} + I \eta_2^{(k+1)}) e^{-\frac{v_3(t)}{2}} \sqrt{s_k} \\ &+ \theta (-1 + J e^{-v_3(t)}) s_k \\ &+ \frac{\theta e^{-\frac{v_3(t)}{2}} (1 + J e^{-v_3(t)}) (I \eta_{02}^{(k+1)} - \rho \chi \eta_{01}^{(k+1)})}{4\sqrt{3}} s_k^{\frac{3}{2}} \\ &+ \frac{\theta \chi^2 J e^{-2v_3(t)}}{24} s_k^2 + \frac{\theta J \chi^4 e^{-3v_3(t)}}{240} s_k^3, \\ {}^t(v_1(0), v_2(0), \log(v_3(0))) &= \tilde{X}_{t_k, x_0}^{(\text{third}, \text{CIR})}, \end{aligned} \quad (13)$$

where $J = \xi - \frac{\chi^2}{4\theta}$, $I = \sqrt{1 - \rho^2} \chi$.

REMARK 6 (A third-order discretization method for the qGSV-CIR model in general $l > 0$ case) Using the algebraic structure (12) and the 7-moment similar family given in Theorem 3.1 of Shinozaki (2017), we can express a third-order method for the general $l > 0$ case as follows. Setting $d = l + 1$ and let $\{\eta_i^{(k)}, \eta_{0i}^{(k)}, \eta_{ij}^{(k)}\}_{i=1 \leq i \leq j \leq d, k=1, \dots, n}$ be a family of independent standard normal random variables. Then, a third order discretization method for the qGSV-CIR is as follows:

$$\begin{aligned} \tilde{X}_{t_0, x_0}^{(\text{third}, \text{CIR})} &= x_0, \\ \tilde{X}_{t_{k+1}, x_0}^{(\text{third}, \text{CIR})} &= \exp \left(\sum_{i=1}^d \eta_i^{(k+1)} V_i^{\text{CIR}} \sqrt{s_k} + V_0^{\text{CIR}} s_k \right. \\ &+ \sum_{1 \leq i \leq j \leq d} \left(\frac{((-1)^j \eta_{0j}^{(k+1)} \eta_i^{(k+1)} + (-1)^{i+1} \eta_{0i}^{(k+1)} \eta_j^{(k+1)} + \eta_{ij}^{(k+1)})}{2\sqrt{3}} [V_i^{\text{CIR}}, V_j^{\text{CIR}}] \right) s_k \\ &+ \sum_{i=1}^d \left(\frac{-\eta_{0i}^{(k+1)}}{2\sqrt{3}} [V_0^{\text{CIR}}, V_i^{\text{CIR}}] s_k^{\frac{3}{2}} + \frac{1}{12} [[V_0^{\text{CIR}}, V_i^{\text{CIR}}], V_i^{\text{CIR}}] s_k^2 \right. \\ &+ \frac{1}{360} [[[[V_0^{\text{CIR}}, V_i^{\text{CIR}}], V_i^{\text{CIR}}], V_i^{\text{CIR}}], V_i^{\text{CIR}}] s_k^3 \Big) \\ &+ \sum_{1 \leq i \leq j \leq d} \frac{1}{180} [[[[V_0^{\text{CIR}}, V_j^{\text{CIR}}], V_j^{\text{CIR}}], V_i^{\text{CIR}}], V_i^{\text{CIR}}] s_k^3 \Big) \\ &\times \left(\tilde{X}_{t_k, x_0}^{(\text{third}, n)} \right). \end{aligned}$$

On the other hand, in the qGSV-EXOU model, we can find an approximate solution as in the N-N method. Let $\tilde{X}_{t_{k+1}, x_0}^{(\text{third}, \text{EXOU}), (i)}$ denotes i -th coordinate of $\tilde{X}_{t_{k+1}, x_0}^{(\text{third}, \text{EXOU})}$, then

$$\begin{aligned} \tilde{X}_{t_{k+1}, x_0}^{(\text{third}, \text{EXOU}), (1)} &= e^{-\kappa s_k} \left(\tilde{X}_{t_k, x_0}^{(\text{third}, \text{EXOU}), (1)} + \tilde{X}_{t_k, x_0}^{(\text{third}, \text{EXOU}), (2)} \frac{1 - e^{-\kappa s_k}}{\kappa} \right) \\ &+ s_k B e^{2\tilde{X}_{t_k, x_0}^{(\text{third}, \text{EXOU}), (3)}} \left(\frac{1}{2} + \frac{\alpha_1 - \kappa s_k}{3} \right. \\ &+ \frac{2\alpha_2 + 4\alpha_1^2 - 6\kappa \alpha_1 s_k + 3\kappa^2 s_k^2}{24} \end{aligned}$$

$$\begin{aligned}
& + \frac{\alpha_3 + 6\alpha_1\alpha_2 + 4\alpha_1^3 - 4\kappa s_k(\alpha_2 + 2\alpha_1^2)}{60} \Bigg) \\
& + \left(A_1 + \frac{A_2 C}{\theta s_k} \right) \exp \left(\tilde{X}_{t_k, x_0}^{(\text{third, EXOU}), (3)} \right) \\
& \times \left(1 + \frac{\alpha_1}{2} + \frac{\alpha_1^2 + \alpha_2}{6} + \frac{\alpha_1^3 + 3\alpha_1\alpha_2 + \alpha_3}{24} \right. \\
& + \frac{\alpha_1^4 + 6\alpha_1^2\alpha_2 + 3\alpha_2^2 + 4\alpha_1\alpha_3 + \alpha_4}{120} \Bigg) \\
& + A_2 \left(\tilde{X}_{t_k, x_0}^{(\text{third, EXOU}), (3)} - \frac{C}{\theta s_k} \right) \exp \left(\tilde{X}_{t_k, x_0}^{(\text{third, EXOU}), (3)} \right) \\
& \left(1 + \frac{\alpha_1 - \theta s_k}{2} + \frac{(\alpha_1 - \theta s_k)(\alpha_1 - \theta s_k) + \alpha_2}{6} \right. \\
& + \frac{(\alpha_1 - \theta s_k)^3 + 3(\alpha_1 - \theta s_k)\alpha_2 + \alpha_3}{24} \\
& + \frac{(\alpha_1 - \theta s_k)^4 + 6(\alpha_1 - \theta s_k)\alpha_2 + 3\alpha_2^2 + 4(\alpha_1 - \theta s_k)\alpha_3 + \alpha_4}{120} \Bigg) \Bigg) + \mathcal{O}(s_k^4),
\end{aligned}$$

$$\begin{aligned}
\tilde{X}_{t_{k+1}, x_0}^{(\text{third, EXOU}), (2)} &= e^{-2\kappa s_k} \left(\tilde{X}_{t_k, x_0}^{(\text{third, EXOU}), (2)} + B e^{2\tilde{X}_{t_k, x_0}^{(\text{third, EXOU}), (3)}} \right. \\
&\times \left(1 + \alpha_1 + \frac{\alpha_2 + 2\alpha_1^2}{3} + \frac{\alpha_3 + 6\alpha_1\alpha_2 + 4\alpha_1^3}{12} \right. \\
&+ \left. \left. \frac{\alpha_4 + 8\alpha_3\alpha_1 + 6\alpha_2^2 + 24\alpha_1^2\alpha_2 + 8\alpha_1^4}{60} \right) \right) + \mathcal{O}(s_k^4), \\
\tilde{X}_{t_{k+1}, x_0}^{(\text{third, EXOU}), (3)} &= \frac{C}{s_k \theta} + \left(\tilde{X}_{t_k, x_0}^{(\text{third, EXOU}), (3)} - \frac{C}{s_k \theta} \right) e^{-s_k \theta}.
\end{aligned}$$

where

$$\begin{aligned}
A_1 &= \eta_1^{(k+1)} \sigma \sqrt{s} \\
&- \frac{\chi \sigma}{2} \left(\rho + \frac{(\eta_{02}^{(k+1)} \eta_1^{(k+1)} + \eta_{01}^{(k+1)}) \sqrt{1 - \rho^2}}{\sqrt{3}} \right) s \\
&+ \left(\frac{\sigma}{2\sqrt{3}} \left(-\eta_{01}^{(k+1)} \left(\theta \xi + \kappa + \frac{\chi^2 \rho^2}{2} \right) \right. \right. \\
&+ \left. \left. \frac{\eta_{02}^{(k+1)} \chi^2 \rho \sqrt{1 - \rho^2}}{2} \right) + \frac{\chi^2 \sqrt{1 - \rho^2} \sigma}{12} \right) \\
&\times \left(-(\eta_2^{(k+1)} + 2\eta_{112}^{(k+1)}) \rho \right. \\
&+ \left. (\eta_1^{(k+1)} + 2\eta_{122}^{(k+1)}) \sqrt{1 - \rho^2} \right) s_k^{\frac{3}{2}}
\end{aligned}$$

$$\begin{aligned}
& + \left(\frac{\chi \rho \sigma (4\theta - 2\theta \xi - 2\kappa - \chi^2)}{24} \right. \\
&- \left. \frac{(\eta_{02}^{(k+1)} \eta_1^{(k+1)} + \eta_{01}^{(k+1)} \eta_2^{(k+1)} + \eta_{12}^{(k+1)}) \chi^3 \sqrt{1 - \rho^2} \sigma}{36\sqrt{3}} \right) s_k^2 \\
&+ \frac{\chi^4 \sigma \sqrt{1 - \rho^2} (\eta_1^{(k+1)} \sqrt{1 - \rho^2} - \rho \eta_2^{(k+1)})}{360} s_k^{\frac{5}{2}} \\
&+ \frac{\chi^3 \sigma \rho (-2(\theta \xi + \kappa) + 2\theta + 6\theta \rho^2 - 2\chi^2 \rho^2 + \chi^2 \rho^4 - (1 - \rho^2)^2)}{720} s_k^3, \\
A_2 &= \frac{\eta_{01}^{(k+1)} \sigma \theta}{2\sqrt{3}} s_k^{\frac{3}{2}} + \frac{\chi \rho \sigma \theta}{12} s_k^2 + \frac{\chi^3 \rho \sigma \theta}{360} s_k^3, \\
B &= \sigma^2 s_k + \frac{(\eta_{01}^{(k+1)} \chi \rho - \eta_{02}^{(k+1)} \chi \sqrt{1 - \rho^2}) \sigma^2}{\sqrt{3}} s_k^{\frac{3}{2}} \\
&+ \frac{\chi^2 \sigma^2}{3} s_k^2 + \frac{2\chi^4 \sigma^2}{45} s_k^3, \\
C &= (\eta_1^{(k+1)} \rho + \eta_2^{(k+1)} \sqrt{1 - \rho^2}) \chi \sqrt{s_k} + \theta * \xi s_k \\
&+ \frac{(-\eta_{01}^{(k+1)} * \rho + \eta_{02}^{(k+1)} \sqrt{1 - \rho^2}) \theta \chi}{2\sqrt{3}} s_k^{\frac{3}{2}}, \\
\alpha_1 &= (\eta_1^{(k+1)} \rho + \eta_2^{(k+1)} \sqrt{1 - \rho^2}) \chi \sqrt{s_k} \\
&+ (\theta \xi + \kappa) s_k + \frac{(-\eta_{01}^{(k+1)} \rho + \eta_{02}^{(k+1)} \sqrt{1 - \rho^2}) \theta \chi}{2\sqrt{3}} s_k^{\frac{3}{2}} \\
&- \theta \tilde{X}_{t_k, x_0}^{(\text{third, EXOU}), (3)} s_k, \\
\alpha_2 &= -(\eta_1^{(k+1)} \rho + \eta_2^{(k+1)} \sqrt{1 - \rho^2}) \chi \sqrt{s} + \theta \xi s_k \\
&+ \frac{(-\eta_{01}^{(k+1)} \rho + \eta_{02}^{(k+1)} \sqrt{1 - \rho^2}) \theta \chi}{2\sqrt{3}} s_k^{\frac{3}{2}} \Bigg) s_k \theta \\
&+ \theta^2 \tilde{X}_{t_k, x_0}^{(\text{third, EXOU}), (3)} s_k^2, \\
\alpha_3 &= (-\tilde{X}_{t_k, x_0}^{(\text{third, EXOU}), (3)} + (\eta_1^{(k+1)} \rho + \eta_2^{(k+1)} \sqrt{1 - \rho^2}) \\
&+ \frac{-\eta_{01}^{(k+1)} \rho + \eta_{02}^{(k+1)} \sqrt{1 - \rho^2}}{2\sqrt{3}}) \chi \sqrt{s_k} + \theta \xi s_k \Bigg) s_k^3 \theta^3.
\end{aligned}$$

Note that $\tilde{X}_{t_{k+1}, x_0}^{(\text{third, EXOU})}$ is an approximate solution at time $t = 1$ to the following ODEs:

$$\begin{aligned}
\frac{d}{dt} v_1(t) &= (v_2(t) - \kappa v_1(t)) s_k + A_1 e^{v_3(t)} + A_2 v_3(t) e^{v_3(t)}, \\
\frac{d}{dt} v_2(t) &= -2\kappa s_k v_2(t) + B e^{v_3(t)}, \\
\frac{d}{dt} v_3(t) &= -s_k \theta v_3(t) + C, \\
{}^t(v_1(0), v_2(0), v_3(0)) &= \tilde{X}_{t_k, x_0}^{(\text{third, EXOU})}.
\end{aligned}$$

4. Numerical result

In this section, using the discretization formulas exhibited in the previous section, we describe the numerical experiments of practically important problems. The problem we challenge is the pricing of a path-dependent interest rate exotic option: so-called *Snowball*.

4.1. Snowball pricing

Snowball is one of the major exotic derivative instruments. From a modeling perspective, this product has strong path-dependence as the coupon C_i at time T_i depends on all previous coupons C_1, C_2, \dots, C_{i-1} ; therefore, the Monte Carlo simulation is mandatory. The coupons of Snowball we deal with is based on an inverse floater as follows:

$$C_0 = 0, \quad C_i = \min\{\max\{C_{i-1} + k - L(T_i, T_{i+1}), f\}, c\},$$

where $L(T_i, T_{i+1})$ is the interest rate at time T_i for the period $[T_i, T_{i+1}]$, k is the margin, f is the floor, and c is the cap of the coupons. The payoff of Snowball whose notional is \mathcal{N} is

$$\begin{aligned} & \mathcal{N} C_i \delta(T_{i-1}, T_i) \quad \text{at } T_i, \\ & \mathcal{N} (C_K \delta(T_{K-1}, T_K) + 1) \quad \text{at maturity } T_K, \end{aligned}$$

where $\delta(T_{i-1}, T_i)$ is the day count of the period $[T_{i-1}, T_i]$.

Let us consider the process $(x(t), y(t), z(t))$ of the qG-SV model (i.e. (7) or (8)). As described in section 3.1, assuming that the fixing lag is zero, we can formulate $L(T_i, T_{i+1})$ as a function of $x(T_i), y(T_i)$, and thereby C_i as a function of $x(T_i), y(T_i)$. In addition, assuming the discount factor is flat, we can represent the price of Snowball under an appropriate pricing measure as follows:

$$E \left[\mathcal{N} \sum_{i=1}^K C_i \delta(T_{i-1}, T_i) + \mathcal{N} \right].$$

Subsequently, for simplicity of exposition, we consider the numerical evaluation of the following expectation which depends only on random variables $\{x(T_i), y(T_i)\}_{i=1, \dots, K}$:

$$\begin{aligned} & E \left[\sum_{i=1}^K C_i \right], \quad \text{where } C_0 = 0, \\ & C_i = \min\{\max\{C_{i-1} + k - L(T_i, T_{i+1}), f\}, c\}. \end{aligned} \quad (14)$$

In the numerical experiments of the next subsection, the terms of Snowball are specified as $K = 10$ (i.e. ten years annual payment), $c = 0.1, f = 0.01, k = 0.6$.

In addition, in the next subsection, we conduct the simulations by partitioning the interval $[T_i, T_{i+1}]$ into n time grids; in other words, we take $n \times K$ time grids to calculate the above expectation. Furthermore, we use the even partitions, i.e.,

$$s_{i,j} = \frac{T_{i+1} - T_i}{n} j + T_i \quad (i = 1, \dots, K, j = 0, 1, \dots, n).$$

As discussed in Remark 4.1 of Shinozaki (2017), this is justified only for the N-V and N-N methods; however, the

numerical results in Shinozaki (2017) empirically show that it also works for the $Q_{(s)}^{(7,2)}$ method.

We first generate a set of random variable $\{\hat{x}^{(\text{method}, n)}(T_i), \hat{y}^{(\text{method}, n)}(T_i)\}_{i=1, \dots, K}$ using one of the discretization methods, then calculate $\hat{L}^{(\text{method}, n)}(T_i, T_{i+1})$ by substituting $\{\hat{x}^{(\text{method}, n)}(T_i), \hat{y}^{(\text{method}, n)}(T_i)\}_{i=1, \dots, K}$ into (5) and (6), thus obtain $\{\hat{C}_i^{(\text{method}, n)}\}_{i=1, \dots, K}$ that approximates $\{C_i\}_{i=1, \dots, K}$. To calculate the integration

$$\hat{E} \left[\sum_{i=1}^K \hat{C}_i^{(\text{method}, n)} \right], \quad (15)$$

we used the Sobol sequences with Kuo's initial number (Joe and Kuo 2003, 2008) with an appropriate sample number M in each case described below.

4.2. Numerical result

Now, we present the numerical results of pricing the Snowball under the qGSV-CIR and qGSV-EXOU models.

4.2.1. Quasi-Gaussian term-structure model with CIR-type stochastic volatility. As described in section 3.3, a closed or approximate solution to the involved ODEs can be found only in the N-V method; numerical methods to solve ODEs are required to implement the N-N and $Q_{(s)}^{(7,2)}$ methods. We use the explicit R-K methods, specifically, a 5-th order R-K method for the N-N method and a 7-th order R-K method for the $Q_{(s)}^{(7,2)}$ method; since a particular accuracy of numerical solutions to the ODEs is necessary to achieve higher-order discretization of the SDE, see Corollary 1.4 and Section 6.2.1 of Ninomiya and Ninomiya (2009).

Setting the parameters in (7) as $\kappa = 0.1, \sigma = 0.02, \theta = 1.5, \xi = \chi = 0.01, \rho = -0.5, z(0) = 0.1$, we consider the true value as follows in this experiment:

$$E \left[\sum_{i=1}^K C_i \right] = 0.01349520829164,$$

this value was estimated using the $Q_{(s)}^{(7,2)}$ method with the number of partitions $n = 20$ and $M = 2^{24}$.

REMARK 7 (True values of numerical experiments) The weak convergences of each methods are stated in propositions 2, 3, 4, respectively, thus we estimate the true values of numerical experiments by using the $Q_{(s)}^{(7,2)}$ method in this paper. Note that, to make assurance double sure, the above mentioned estimated value is validated by matching the values calculated by another method up to a certain digit, specifically the difference between the estimated values using the $Q_{(s)}^{(7,2)}$ and the N-V methods with the Romberg extrapolation where $n = 20, M = 2^{24}$ is under 10^{-9} .

The relations between the discretization error $|\hat{E}[\sum_{i=1}^K \hat{C}_i^{(\text{method}, n)}] - E[\sum_{i=1}^K C_i]|$ and the number n of partitions of each method are plotted in Figure 1. In addition to the higher-order methods that exhibited in the previous section, the discretization errors of the conventional E-M method and the quadratic-exponential (QE) method which matches moments

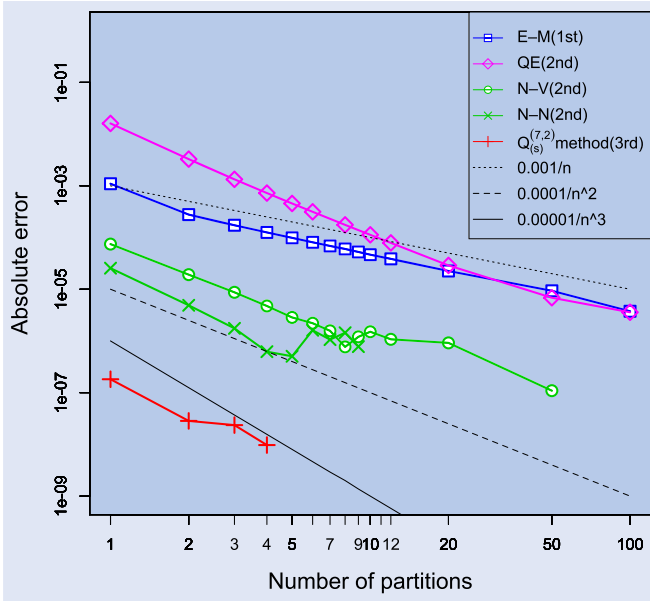


Figure 1. Discretization error (qGSVCIR).

up to the 2nd order are plotted. Here, to approximate the integration (15), we used the Sobol sequence with the number of sample points $M = 2^{22}$, which assures enough accuracy to neglect the integration error compared to the levels of the discretization errors.

Figure 1 indicates that the theoretical orders can be obtained using each method. Moreover, $C^{(EM)} \gg C^{(NV)} > C^{(NN)} \gg C^{(Third)}$ holds in this case; this is the same as the numerical experiments described in Shinozaki (2017). On the other hand, $C^{(QE)}$, that is the discretization error of the QE method with $n = 1$, is somewhat large in our experiment.

To compare the performance of each method, Table 1 summarizes the requirements to obtain 10^{-6} , (i.e. 0.01 bp accuracy); that are the number n of partitions, the number M of sample points of the quasi-Monte Carlo method, the number $D(n)$ of dimensions of integration (15), the number $E(n)$ of ODEs to be solved to generate one sample path of (15), the methods to solve ODEs, and the amount of computation time. Note that $D(n) = D^{(method)}(n) \times K$, $E(n) = E^{(method)}(n) \times K$ where $D^{(method)}(n)$, $E^{(method)}(n)$ for each method are described in remark 2, CPU time is in seconds; the CPU used in the experiments of this paper is Intel Core i5 (2.3 GHz).

It is evident that the higher-order methods enable much faster computation. As explained in section 2.2, a higher-order method enables the reduction of n and thereby $D(n)$, $E(n)$, by improving the order and a constant, $C^{(method)}$ as discussed. In addition, M can be reduced, because the smaller

$D(n)$ becomes, the faster the convergence of the quasi-Monte Carlo becomes. Reductions of n , M , and $E(n)$ enable much faster computation, as the CPU times of each method show.

Furthermore, it should be emphasized that, in our case, a higher-order method even more drastically reduces the computational costs compared to the numerical experiments described in Shinozaki (2017). This is because the high-dimensionality of the problem, that is, $D(n)$ and $E(n)$ are larger in our case since the payoff of Snowball depends on K points of time. The payoff of derivative product whose price needs to be calculated numerically usually depends on multiple times, hence the higher-order methods have the potential to improve computational costs of many practical problems. In fact, the $Q_{(s)}^{(7,2)}$ method is more than 5000 times faster than the conventional E-M method in this example. It may also be worth mentioning here that the N-V method is faster than the N-N method, despite the fact that n , M , and $D(n)$ are larger in the N-V method; this is because the closed-form solution is available in the N-V method for qGSV-CIR as discussed.

REMARK 8 (Setting of volatility χ of CIR process) As described, we set $\chi = 0.01$ in our experiment in order to avoid a square root of a negative number in the simulation by ensuring $J = \xi - \frac{\chi^2}{4\theta} > 0$. Note that the N-V method (9) is not well defined $J = \xi - \frac{\chi^2}{4\theta} < 0$; see Remark 4.7 of Shinozaki (2017) for more detail. In practice, to fit the volatility smiles to observed market prices, χ is often set to be a more larger value; as a result, this condition can be unsatisfied. To deal this problem, we can use the QE method or the extensions of higher-order methods such as proposed in Alfonsi (2010). Note that this kind of problem cannot occur in the qGSV-EXOU model discussed in the next subsection.

4.2.2. Quasi-Gaussian term-structure model with exponential Ornstein-Uhlenbeck-type stochastic volatility. For the qGSV-EXOU model, we can construct approximate solutions to the involved ODEs in the N-V, N-N, $Q_{(s)}^{(7,2)}$ methods; therefore, the higher-order methods are easier to implement compared with the case of the qGSV-CIR model. Setting the parameters in (8) as $\kappa = 0.1$, $\sigma = 0.02$, $\theta = 1.2$, $\xi = 0.01$, $\chi = 0.1$, $\rho = -0.5$, $z(0) = 0.01$, we consider the true value as follows in this experiment:

$$E \left[\sum_{i=1}^K C_i \right] = 0.2207549319733,$$

this value was estimated using the $Q_{(s)}^{(7,2)}$ method with the number of partitions $n = 20$ and $M = 2^{27}$.

Table 1. Requirements for 10^{-6} accuracy in case of the qGSV-CIR model.

Method	n	M	$D(n)$	$E(n)$	ODE solver	CPU time
E-M	201	3.0×10^6	$201 \times 2 \times 10$	—	—	5410
N-V	9	5.0×10^5	$9 \times 3 \times 10$	$9 \times 4 \times 10$	Closed	23.2
N-N	4	8.0×10^4	$4 \times 4 \times 10$	$4 \times 2 \times 10$	5-th R-K	50.4
$Q_{(s)}^{(7,2)}$	1	1.3×10^4	$1 \times 5 \times 10$	$1 \times 1 \times 10$	7-th R-K	0.97

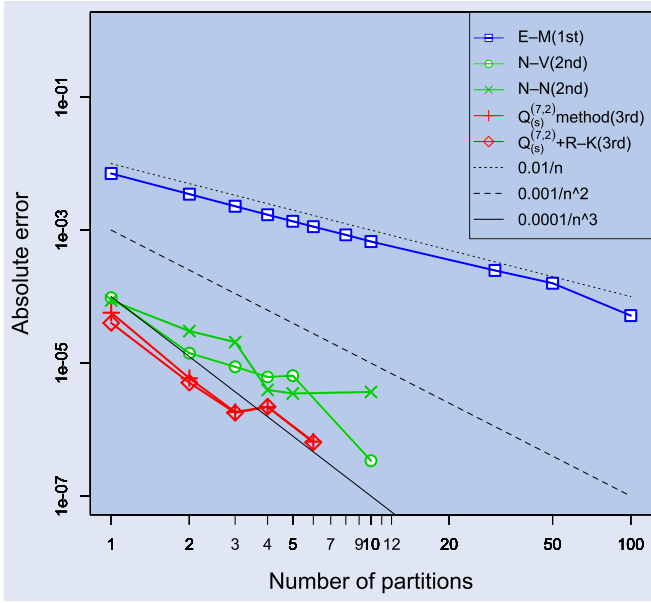


Figure 2. Discretization error (qGSV-EXOU).

The relations between the discretization error $|\hat{E}[\sum_{i=1}^K \hat{C}_i^{(\text{method},n)}] - E[\sum_{i=1}^K C_i]|$ and the number n of partitions of each method are plotted in Figure 2. In addition to the E-M, N-V, N-N, and $Q_{(s)}^{(7,2)}$ methods, the discretization errors of the $Q_{(s)}^{(7,2)}$ method using the 7-th R-K method for solving ODEs are plotted. Here, to approximate the integration (15), we used the Sobol sequence with the number of sample points $M = 2^{22}$, which assures enough accuracy to neglect the integration error compared to the levels of the discretization errors. Figure 2 also indicates that the theoretical orders can be obtained using each method.

Moreover, Tables 2 and 3 summarize the requirements to obtain 10^{-4} (i.e. 1 bp accuracy) and 10^{-5} (i.e. 0.1 bp accuracy), respectively. It is evident that the higher-order methods enable much faster computation as same in the qGSV-CIR case. To obtain 10^{-4} accuracy, which is often required in practice, we need to set $n = 79$ (i.e. take time grids for every several days) in the conventional E-M method; however, we need only $n = 1$ (i.e. take time grids for every year)

in the $Q_{(s)}^{(7,2)}$ method. We also mention here that the higher-order methods are more time-saving when more accuracy is required; in fact, to obtain 10^{-5} accuracy, the $Q_{(s)}^{(7,2)}$ method is more than 6,000 times faster than the E-M method, although only about 500 times faster in the case of 10^{-4} accuracy as demonstrated. In addition, note that the $Q_{(s)}^{(7,2)}$ method with the approximation solutions is only about 2 times faster than the $Q_{(s)}^{(7,2)}$ method with the R-K method; however, the explicit higher-order discretization method is much more preferable in the practical implementation.

REMARK 9 (Other parameter settings) In practice, more flexible parameter settings are often required, e.g. the mean reversion κ and the volatility σ are time-dependent, the volatility σ and the volatility of volatility χ are often set to be larger. To apply the proposed methods in the case of time-dependent parameters, some further discussions are necessary, which is our future work.

On the other hand, the proposed methods are still applicable in high volatility cases. Resetting $\sigma = 0.2$, $\chi = 0.8$, $z(0) = 0.1$, we conduct the numerical experiment of the qGSV-EXOU model. The relations between the discretization error $|\hat{E}[\sum_{i=1}^K \hat{C}_i^{(\text{method},n)}] - E[\sum_{i=1}^K C_i]|$ and the number n of partitions of each method are plotted in Figure 3.

5. Concluding remark

The numerical results of the previous section show that the KLVN-scheme is even more efficient for the practical high-dimensional problems, especially for the case the close or approximate solutions to the involved ODEs can be found, such as the qGSV-EXOU model. Although the qGSV-CIR model is somewhat popular among practitioners and its practical issues are discussed, for example, in Anderson and Piterbarg (2010), the qGSV-EXOU is not. To use the qGSV-EXOU in practice, we need to develop techniques for solving practical issues such as calibration procedure, parameter setting to provide better fits to the volatility smiles, and stable Greeks calculations, etc.; they shall be our next challenges.

Table 2. Requirements for 10^{-4} accuracy in case of the qGSV-EXOU model.

Method	n	M	$D(n)$	$E(n)$	ODE solver	CPU time
E-M	79	$2^{20} \approx 1.05 \times 10^6$	$64 \times 2 \times 10$	—	—	451
N-V	2	5.3×10^3	$2 \times 3 \times 10$	$2 \times 4 \times 10$	Approx	2.68
N-N	2	1.1×10^4	$2 \times 4 \times 10$	$2 \times 2 \times 10$	Approx	11.76
$Q_{(s)}^{(7,2)}$	1	2.1×10^3	$1 \times 7 \times 10$	$1 \times 1 \times 10$	Approx	0.95
$Q_{(s)}^{(7,2)} + \text{R-K}$	1	2.1×10^3	$1 \times 7 \times 10$	$1 \times 1 \times 10$	7-th R-K	1.46

Table 3. Requirements for 10^{-5} accuracy in case of the qGSV-EXOU model.

Method	n	M	$D(n)$	$E(n)$	ODE solver	CPU time
E-M	587	$2^{22} \approx 4.19 \times 10^6$	$587 \times 2 \times 10$	—	—	45,523
N-V	4	1.8×10^4	$4 \times 3 \times 10$	$4 \times 4 \times 10$	Approx	13.59
N-N	4	6.5×10^4	$4 \times 4 \times 10$	$4 \times 2 \times 10$	Approx	43.80
$Q_{(s)}^{(7,2)}$	2	1.2×10^4	$2 \times 7 \times 10$	$2 \times 1 \times 10$	Approx	6.89
$Q_{(s)}^{(7,2)} + \text{R-K}$	2	1.2×10^4	$2 \times 7 \times 10$	$2 \times 1 \times 10$	7-th R-K	12.69

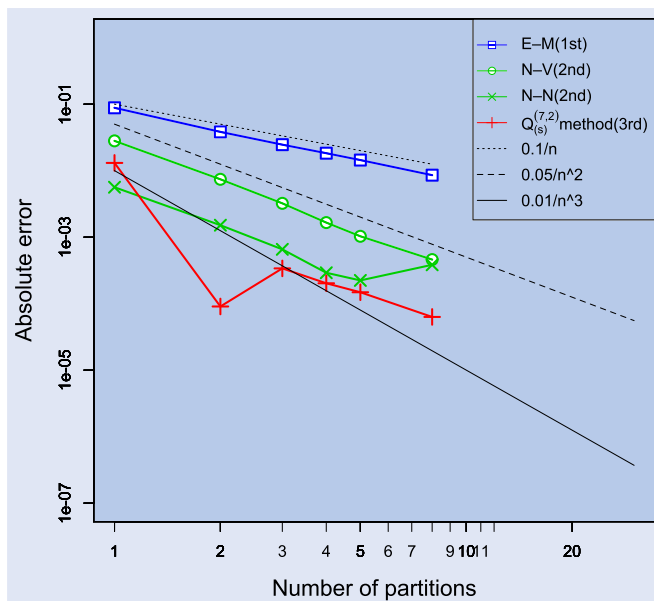


Figure 3. Discretization error (qGSV-EXOU; High volatilities).

Acknowledgments

I am most grateful to my former commercial supervisor Dr. Yasufumi Osajima (SMBC Nikko Securities Inc) for suggesting the topic treated in this paper and hope to collaborate with him on the next challenges. I also thank Prof. Syoiti Ninomiya (Tokyo Institute of Technology) and my former colleagues Takehiro Fujiwara, Ryo Asano (SMBC Nikko Securities Inc) for their valuable comments and continuous encouragement.

Disclosure statement

No potential conflict of interest was reported by the authors.

References

- Ahdida, A., Alfonsi, A. and Palidda, E., Smile with the Gaussian term structure model. *J. Comput. Finance*, 2017, **21**(1), 115–167.
- Alfonsi, A., High order discretization schemes for the CIR process: Application to affine term structure and Heston models. *Math. Comput.*, 2010, **79**(269), 209–237.
- Andersen, L., Simple and efficient simulation of the heston stochastic volatility model. *J. Comput. Finance*, 2008, **11**(3), 1–43.
- Andersen, L. and Piterbarg, V., *Interest Rate Modeling*, Vol. 1–3, 2010 (Atlantic Financial Press: London, New York).
- Andreasen, J., Turbo charging the cheyette model. Available at SSRN 1719142, 2001.
- Andreasen, J., Markovian term structure models. *Encyclopedia Quant. Finance*, 2010, **III**, 1159–1164.
- Bally, V. and Talay, D., The law of the Euler scheme for stochastic differential equations. *Probab. Theory. Relat. Fields*, 1996, **104**(1), 43–60.
- Barndorff-Nielsen, O.E. and Shephard, N., Modelling by lévy processes for financial econometrics. In *Lévy Processes*, pp. 283–318 (Springer), 2001a.
- Barndorff-Nielsen, O.E. and Shephard, N., Non-Gaussian Ornstein–Uhlenbeck-based models and some of their uses in financial economics. *J. R. Stat. Soc. Ser. B (Stat. Methodol.)*, 2001b, **63**(2), 167–241.
- Bayer, C., Friz, P. and Loeffen, R., *Semi-closed form cubature and applications to financial diffusion models*. *Quant. Finance*, 2013, **13**(5), 769–782.
- Beyna, I., *Interest Rate Derivatives: Valuation, Calibration and Sensitivity Analysis*, 2013 (Springer Science & Business Media: Berlin, Heidelberg).
- Brace, A., Gatarek, D. and Musiela, M., The market model of interest rate dynamics. *Math. Finance*, 1997, **7**(2), 127–155.
- Cheyette, O., Markov representation of the Heath-Jarrow-Morton model. BARRA Working Paper, 1991.
- Cox, J.C., Ingersoll, J.E. and Ross, S.A., A theory of the term structure of interest rates. *Econometrica*, 1985, **53**(2), 385–407.
- Crisan, D. and Manolarakis, K., Solving backward stochastic differential equations using the cubature method: Application to nonlinear pricing. *SIAM J. Financ. Math.*, 2012, **3**(1), 534–571.
- Crisan, D. and Manolarakis, K., Second order discretization of backward SDEs and simulation with the cubature method. *Ann. Appl. Probab.*, 2014, **24**(2), 652–678.
- Duffy, D.J., *Finite Difference Methods in Financial Engineering: A Partial Differential Equation Approach*, 2013 (John Wiley & Sons: Chichester).
- Fujiwara, T., *Sixth Order Methods of Kusuoka Approximation*. Preprint Series, Graduate School of Mathematical Sciences, Univ. Tokyo, 2006.
- Glasserman, P., *Monte Carlo Methods in Financial Engineering*, Vol. 53, 2013 (Springer Science & Business Media: New York).
- Green, A., *XVA: Credit, Funding and Capital Valuation Adjustments*, 2015 (Wiley: Hoboken, NJ).
- Gregory, J., *The xVA Challenge: Counterparty Credit Risk, Funding, Collateral, and Capital*, 3rd ed., 2015 (Wiley: New York).
- Heath, D., Jarrow, R. and Morton, A., Bond pricing and the term structure of interest rates: A new methodology for contingent claims valuation. *Econom. J. Econom. Soc.*, 1992, **60**, 77–105.
- Ho, T.S. and Lee, S.-B., Term structure movements and pricing interest rate contingent claims. *J. Finance*, 1986, **41**(5), 1011–1029.
- Hull, J. and White, A., Pricing interest-rate-derivative securities. *Rev. Financ. Stud.*, 1990, **3**(4), 573–592.
- Hunt, P., Kennedy, J. and Pelsser, A., Markov-functional interest rate models. *Financ. Stoch.*, 2000, **4**(4), 391–408.
- Jamshidian, F., Bond option evaluation in the Gaussian interest rate model. *Res. Finance*, 1991, **9**, 131–170.
- Joe, S. and Kuo, F., Remark on algorithm 659: Implementing Sobol’s quasirandom sequence generator. *ACM Trans. Math. Softw. TOMS*, 2003, **29**(1), 49–57.
- Joe, S. and Kuo, F., Constructing {S}obol sequences with better two-dimensional projections. *SIAM. J. Sci. Comput.*, 2008, **30**(5), 2635–2654.
- Kloeden, P. and Platen, E., *Numerical Solution of Stochastic Differential Equations*, 1999 (Springer: Berlin).
- Kusuoka, S., Approximation of expectation of diffusion process and mathematical finance. In *Proceedings of Final Taniguchi Symposium, Nara*, Vol. 31 of Advanced Studies in Pure Mathematics, pp. 147–165, 2001.
- Kusuoka, S., Malliavin calculus revisited. *J. Math. Sci. Univ. Tokyo*, 2003, **10**(2), 261–277.
- Kusuoka, S., Approximation of expectation of diffusion processes based on Lie algebra and Malliavin calculus. *Adv. Math. Econom.*, 2004, **6**, 69–83.
- Kusuoka, S., Gaussian K-scheme: Justification for KLVN method. *Adv. Math. Econom.*, 2013, **17**, 71–120.
- Lyons, T. and Victoir, N., Cubature on wiener space. In *Proceedings of the Royal Society of London A: Mathematical, Physical and Engineering Sciences*, Vol. 460, pp. 169–198, 2004.
- Maruyama, G., Continuous Markov processes and stochastic equations. *Rendiconti del Circolo Matematico di Palermo*, 1955, **4**(1), 48.
- Milstein, G., Approximate integration of stochastic differential equations. *Theory Probab. Appl.*, 1975, **19**(3), 557–562.
- Morimoto, Y. and Sasada, M., *Algebraic structure of vector fields in financial diffusion models and its applications*. *Quant. Finance*, 2017, **17**(7), 1105–1117.

- Nicolato, E. and Venardos, E., Option pricing in stochastic volatility models of the Ornstein-Uhlenbeck type. *Math. Finance: Int. J. Math. Stat. Financ. Econom.*, 2003, **13**(4), 445–466.
- Niederreiter, H., *Random Number Generation and Quasi-Monte Carlo Methods*, 1992 (Philadelphia: SIAM).
- Ninomiya, S., A new simulation scheme of diffusion processes: Application of the Kusuoka approximation to finance problems. *Math. Comput. Simul.*, 2003, **62**(3), 479–486.
- Ninomiya, M. and Ninomiya, S., A new higher-order weak approximation scheme for stochastic differential equations and the Runge–Kutta method. *Finance Stoch.*, 2009, **13**(3), 415–443.
- Ninomiya, S. and Shinozaki, Y., Higher-order discretization methods of forward-backward SDEs using KLVN-scheme and their applications to XVA pricing. *Appl. Math. Finance*, 2019, **26**(3), 257–292.
- Ninomiya, S. and Victoir, N., Weak approximation of stochastic differential equations and application to derivative pricing. *Appl. Math. Finance*, 2008, **15**(2), 107–121.
- Oshima, K., Teichmann, J. and Velušček, D., A new extrapolation method for weak approximation schemes with applications. *Ann. Appl. Probab.*, 2012, **22**(3), 1008–1045.
- Perelló, J., Sircar, R. and Masoliver, J., Option pricing under stochastic volatility: The exponential Ornstein–Uhlenbeck model. *J. Stat. Mech. Theory Experiment*, 2008, **2008**(06), P06010.
- Ritchken, P. and Sankarasubramanian, L., Volatility structures of forward rates and the dynamics of the term structure 1. *Math. Finance*, 1995, **5**(1), 55–72.
- Shinozaki, Y., Higher order K-scheme and application to derivative pricing. In Proceedings of the 47th ISCIE International Symposium on Stochastic Systems Theory and Its Applications (Dec. 2015, Honolulu), pp. 137–143, 2016.
- Shinozaki, Y., Construction of a third-order K-scheme and its application to financial models. *SIAM J. Financ. Math.*, 2017, **8**(1), 901–932.
- Talay, D. and Tubaro, L., Expansion of the global error for numerical schemes solving stochastic differential equations. *Stoch. Anal. Appl.*, 1990, **8**(4), 483–509.
- UK Financial Conduct Authority, The future of LIBOR. 2019. <https://www.fca.org.uk/news/speeches/the-future-of-libor>,
- Vasicek, O., An equilibrium characterization of the term structure. *J. Financ. Econ.*, 1977, **5**(2), 177–188.